Human Molecular Genetics, 2005, Vol. 14, No. 3 **357–372**
doi:10.1093/hmg/ddi032
Advance Access published on December 8, 2004

Inactivation of *Drosophila Apaf-1 related killer* suppresses formation of polyglutamine aggregates and blocks polyglutamine pathogenesis

Tzu-Kang Sang[1], Chenjian Li[5], Wencheng Liu[5], Antony Rodriguez[6,†], John M. Abrams[6], S. Lawrence Zipursky[2,3] and George R. Jackson[1,3,4,*]

[1]Neurogenetics Program, Department of Neurology, [2]Department of Biological Chemistry and Howard Hughes Medical Institute, [3]Brain Research Institute, [4]Center for Neurobehavioral Genetics, Neuropsychiatric Institute, David Geffen School of Medicine at UCLA, Los Angeles, CA 90095, USA, [5]Department of Neurology and Neuroscience, Weill Medical College of Cornell University, New York, NY 10021, USA and [6]Department of Cell Biology, University of Texas Southwestern Medical Center, Dallas, TX 75390, USA

Received September 7, 2004; Revised November 10, 2004; Accepted November 26, 2004

Huntington's disease (HD) is caused by expansion of a polyglutamine tract near the N-terminal of huntingtin. Mutant huntingtin forms aggregates in striatum and cortex, where extensive cell death occurs. We used a *Drosophila* polyglutamine peptide model to assess the role of specific cell death regulators in polyglutamine-induced cell death. Here, we report that polyglutamine-induced cell death was dramatically suppressed in flies lacking Dark, the fly homolog of human Apaf-1, a key regulator of apoptosis. Dark appeared to play a role in the accumulation of polyglutamine-containing aggregates. Suppression of cell death, caspase activation and aggregate formation were also observed when mutant huntingtin exon 1 was expressed in homozygous *dark* mutant animals. Expanded polyglutamine induced a marked increase in expression of Dark, and Dark was observed to colocalize with ubiquitinated protein aggregates. Apaf-1 also was found to colocalize with huntingtin-containing aggregates in a murine model and HD brain, suggesting a common role for Dark/Apaf-1 in polyglutamine pathogenesis in invertebrates, mice and man. These findings suggest that limiting Apaf-1 activity may alleviate both pathological protein aggregation and neuronal cell death in HD.

INTRODUCTION

Huntington's disease (HD) is a fully penetrant autosomal-dominant neurodegenerative disorder characterized by chorea, dementia and affective changes (1). HD is caused by expansion of an unstable CAG tract within exon 1 of the huntingtin gene, resulting in expression of an expanded polyglutamine tract near the N-terminal of huntingtin (2,3).There are at least nine other neurodegenerative disorders associated with expansion of polyglutamine, including autosomal dominant spinocerebellar ataxias (SCA1, SCA2, Machado–Joseph disease/SCA3, SCA6, SCA7, SCA12 and SCA17), spinobulbar muscular atrophy and dentatorubral-pallidoluysian atrophy (4,5), suggesting that proteins containing expanded polyglutamine are cytotoxic. Post-mortem examination of HD brain shows neuronal loss in the striatum and cortex (6), with cytoplasmic and nuclear protein aggregates containing N-terminal fragments of mutant huntingtin (7,8). Although molecular pathways leading to neuronal cell death in polyglutamine disease are yet to be completely elucidated, recent studies in HD brain and murine models have identified caspase-dependent proteolytic processes associated with the appearance of insoluble N-terminal huntingtin fragments, suggesting that activation of caspases plays a role in early phases of HD pathogenesis (9,10).

Activation of caspase-8, caspase-3 and caspase-6 is observed in HD striatum (9–11). In cell culture models, expression of polyglutamine-containing proteins affects expression, activation and activity of caspases (11–23). Caspase-2 immunoprecipitates with polyglutamine-expanded huntingtin in an apoptosome-like complex (9). A number of reports have demonstrated that inhibition of caspase activity ameliorates

*To whom correspondence should be addressed at: Neurogenetics Program, Department of Neurology, 710 Westwood Plaza, David Geffen School of Medicine at UCLA, Los Angeles, CA 90095, USA. Tel: +1 3107945638; Fax: +1 3102672473; Email: grjackson@mednet.ucla.edu
†Present address: The Wellcome Trust Genome Campus, Wellcome Trust Sanger Institute, Cambridge CB10 1SA, UK.

polyglutamine-induced phenotypes in HD models. Expression of a dominant negative caspase-1 transgene reduces phenotypic severity and delays mortality in the R6/2 HD mouse (24). Intrathecal infusion of a broad spectrum caspase inhibitor delays mortality in this model (25). The antibiotic minocycline moderately inhibits mutant huntingtin-induced expression of caspase-1 and caspase-3, and delays mortality of the R6/2 mouse (24). Expression of p35, a broad spectrum caspase inhibitor, does not attenuate neuronal degeneration in a fly model of HD (26), and poorly suppresses an eye phenotype resulting from overexpression of an expanded polyglutamine-containing form of ataxin-3 (27). Together, these reports demonstrate that constraints upon caspase activity effectively slow disease progression, although the effects described are generally mild. However, a direct effect of caspase inhibition on cell survival has not been demonstrated.

The accumulation of polyglutamine-containing cytoplasmic and nuclear protein aggregates is a pathological hallmark of HD. Although a large body of circumstantial evidence links cellular toxicity to polyglutamine aggregates, questions as to whether such aggregates are directly pathogenic or simply a byproduct of sick cells remain unsettled. A conditional HD mouse model has demonstrated that blocking expression of mutant huntingtin exon 1, resulting in clearance of aggregates, reverses neuropathology and motor dysfunction (28). The molecular chaperones hsp70 and hsp40 decrease mutant huntingtin toxicity by suppressing the formation of insoluble polyglutamine-containing aggregates *in vitro* and in a yeast HD model (29–31). Several small molecule inhibitors and intracellular peptides that affect aggregate formation have been shown to reduce cell death induced by mutant huntingtin in both culture and animal models (32–35). Taken together, these observations support the contention that expanded polyglutamine aggregates are cytotoxic, and thus that prevention of aggregation is a valid therapeutic approach.

As several molecular components of programed cell death pathways are well defined and hence provide tractable therapeutic targets, we set out to assess their roles in polyglutamine-induced cell death. Here, we used a genetic approach to evaluate candidate modifiers in a fly model expressing an expanded polyglutamine peptide (36) and identified the *Drosophila* Apaf-1-related killer (*dark*) (37), a gene encoding the fly homolog of mammalian Apaf-1 and the *Caenorhabditis elegans* cell death pathway gene CED-4, as an essential effector required for polyglutamine-induced neurodegeneration and, interestingly, polyglutamine aggregation. Dark/Apaf-1 promotes caspase activation through the formation of a caspase complex, the apoptosome (38). Mammalian Apaf-1 is thought to act as a molecular scaffold that links cellular stress via cytochrome *c* release from mitochondria to activation of caspase-9. A conformational change of Apaf-1 occurs when cytochrome *c* binds to the C-terminal WD40 repeats. This is followed by dATP/ATP binding, formation of Apaf-1 multimers and association of procaspase-9 to form the apoptosome. Mutations in *dark* have been identified previously as suppressors of misexpressed cell death genes (i.e. *reaper*, *hid* and *grim*) in the retina (37,39,40). We demonstrated that polyglutamine expression induced, caspase-3-like activity and this activation was suppressed by *dark* mutation. Dark participated in both developmental and adult-onset cell death induced by polyglutamine. Suppression of cell death, caspase activation and aggregate formation were also observed when expanded polyglutamine was expressed within the context of mutant huntingtin exon 1. Ultrastructural analysis suggested that Dark/Apaf-1 plays a role, directly or indirectly, in aggregate formation and toxicity, and is required for the 'dark cell death' previously described in HD models and human brain. Expanded polyglutamine and mutant huntingtin exon 1 were associated with increased Dark expression. Colocalization of Dark/Apaf-1 with protein aggregates was observed in the fly polyglutamine peptide model, the R6/2 mouse model and HD brain, suggesting a conserved phylogenetic role for Dark/Apaf-1 in polyglutamine pathogenesis. The robust suppression of polyglutamine toxicity by mutation of Dark/Apaf-1, as opposed to the mild or no effects of caspase inhibitors in fly and other models, argues that Apaf-1 plays a role in HD pathogenesis that may be, at least in part, caspase-independent.

RESULTS

Mutation of *dark* suppresses developmental polyglutamine-induced cell death

The GAL4/UAS system (41) (Fig. 1A) was used to express a polypeptide containing 108 glutamines (MRSRKL-Q43-R-Q65-KLRS). Expression of UAS-Q108 in all cell types of the eye using the GMR-GAL4 transgene (hereafter referred to as GMR-GAL4:UAS-Q108) resulted in severe degeneration of the retina (Fig. 1D, E and H). The internal structure of the retina was completely disrupted, producing a marked reduction in the size and number of individual rhabdomeres, the organelles responsible for phototransduction within photoreceptor neurons (Fig. 1E and arrow in H). Examination of late pupal eye ultrastructure revealed 'dark' photoreceptor neurons containing abundant electron dense nuclear and cytoplasmic particles (Fig. 1H). Such 'dark cell' changes have been described previously in fly and mouse models of HD, as well as HD brain (26,42,43). In contrast, the GMR-GAL4:UAS-Q108 phenotype was dramatically suppressed in a genetic background containing the homozygous mutation $dark^{CD4}$, a strong hypomorphic allele (37). Morphology of the GMR-GAL4:UAS-Q108 eye was essentially wild-type in a mutant *dark* background ($dark^{CD4}/dark^{CD4}$) (Fig. 1F, G and I). The apparent relationship between 'dark cell death' and *dark* mutations is semantic and coincidental.

Detailed ultrastructural examination of the GMR-GAL4:UAS-Q108 retina revealed numerous abnormal condensed nuclei featuring condensed chromatin crescents (44), a typical characteristic of apoptosis (Supplementary Material, Fig. S1A and B). We also observed a large number of vacuoles in degenerated photoreceptors. In some cases, electron dense granules larger than normal ribosomes were observed dispersed throughout the cytoplasm and congregating around lipid droplet-like structures (Supplementary Material, Fig. S1C). Electron dense endoplasmic reticulum (ER) and mitochondria exhibiting a darkened matrix were frequently identified in degenerating photoreceptor neurons (Supplementary Material, Fig. S1D and E). Numerous electron

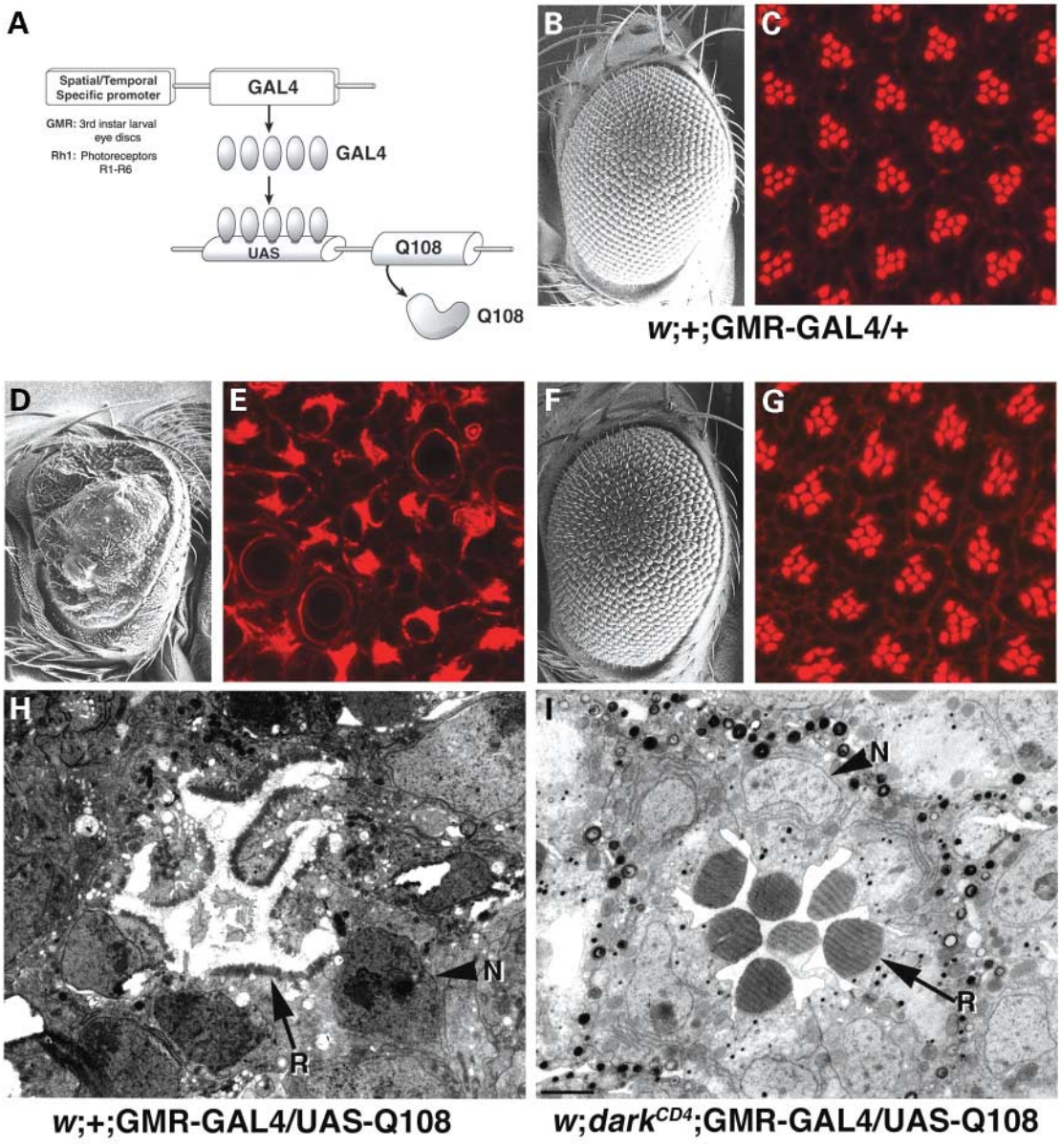

Figure 1. The *dark*^{CD4} mutation suppresses polyglutamine-induced degeneration in the eye. (**A**) Schematic representation of the GAL4/UAS system used to express Q108. (**B** and **C**) Control GMR-GAL4 eyes assessed by SEM (B) and phalloidin staining (C). (**D**, **E** and **H**) GMR-GAL4:UAS-Q108 expression causes retinal neurodegeneration. (D) A severely degenerated eye is seen in this SEM image of a newly eclosed fly. (E) Confocal image of an eye at 90% pupal development stained with phalloidin reveals massive loss of cells and severe tissue disorganization. (H) Electron micrograph of a GMR-GAL4: UAS-Q108 late pupal eye demonstrating 'dark' photoreceptor neurons with severely degenerated rhabdomeres (arrow) and electron dense nuclei (arrowhead). (**F**, **G** and **I**) GMR-GAL4:UAS-Q108 degeneration is suppressed in a homozygous *dark*^{CD4} mutant background. (F) An essentially normal adult eye is seen in this SEM image. (G) Confocal image of an eye at 90% pupal development stained with phalloidin demonstrating a largely normal trapezoidal array of rhabdomeres. (I) Electron micrograph of a *dark*^{CD4}; GMR-GAL4:UAS-Q108 late pupal retina showing normal photoreceptor ultrastructure. The electron dense bodies contain pigment and are normal. Scale bars: B, D, and F, 100 μm. C, E, and G, 5 μm. H and I, 2.5 μm. Labels: (H and I), N, nucleus; R, rhabdomere. Genotypes: (B and C), *w*; +; GMR-GAL4/+. (D, E and H), *w*; +; GMR-GAL4/UAS-Q108-12. (F, G and I), *w*; *dark*^{CD4}; GMR-GAL4/UAS-Q108-12.

dense autophagosomes that appeared to have engulfed ER, nuclei and other subcellular organelles were also identified (Supplementary Material, Fig. S1F), suggesting that autophagy is a component of the cell death associated with expanded polyglutamine, consistent with observations of other investigators (45,46). None of these structures were ever observed when GMR-GAL4:UAS-Q108 was expressed in a background homozygous for the mutant *dark*^{CD4} allele. Electron micrographs revealed normal rhabdomeres and other cellular structures (Fig. 1I).

We tested a number of other mutant *dark* alleles, including the null alleles *dark*^{102} and *dark*^{82} (47). We also tested the parental P element line k11502, as well as *dark*^{DD1}, both weak hypomorphic alleles, for suppression (37). Only strong hypomorphic or null alleles (*dark*^{CD4}, *dark*^{102} and *dark*^{82}) rescued GMR-GAL4:UAS-Q108-induced degeneration in

trans to $dark^{CD4}$ (Supplementary Material, Fig. S2). These data argue that the observed suppression is not due to background mutations in the parental k11502 chromosome.

The *Drosophila* genome encodes seven caspases, including three likely apical caspases (Dredd, Dronc and Strica), as well as four effector caspases (Dcp-1, Drice, Decay and Damm) (48). We evaluated a number of candidate regulators of programed cell death for their effects on degeneration, including GMR-GAL4-targeted expression of p35 (49), and two dominant negative versions of the activator caspase Dronc, UAS-$Dronc^{C318A}$ and UAS-$Dronc^{CARD}$ (50). We also examined the effects of homozygous mutations in *dredd* ($dredd^{D3}$ and $dredd^{B118}$), a gene encoding a protein similar to caspase-8 (51,52). None of these genetic manipulations showed substantial rescue of the GMR-GAL4:UAS-Q108 phenotype.

Mutation in *dark* suppresses apoptosis and caspase activation

Cell death was examined in GMR-GAL4:UAS-Q108 eyes in controls and $dark^{CD4}$ homozygous mutants (Fig. 2). In third instar larval eye discs, just after GMR-GAL4:UAS-Q108 expression commenced, acridine orange staining (53), an indicator of cell death, was identical in control and mutant backgrounds (data not shown). Staining in the GMR-GAL4:UAS-Q108 eye disc was elevated from 40% pupal development to the adult (compare Fig. 2B and with in E control Fig. 2A and D); this staining was strongly suppressed in animals homozygous for mutant *dark* (Fig. 2C and F). Hence, polyglutamine-induced cell death occurs via a Dark-dependent pathway.

Apaf-1 promotes caspase activation through the formation of apoptosome, a holoenzyme complex that accounts for the subsequent activation of caspase-3 and initiation of the execution phase of apoptosis. To directly examine caspase activity, we used a fluorigenic substrate to detect caspase 3-like activity in developing eyes *in situ.* At 60% pupal development, robust caspase-3-like activity was observed in GMR-GAL4:UAS-Q108 eyes (Fig. 2H) but not in controls (Fig. 2G). Consistent with this finding, an antibody to activated Drice (54), a *Drosophila* caspase-3 homolog, showed robust staining in GMR-GAL4:UAS-Q108 eyes (compare Fig. 2K with control in Fig. 2J). Caspase-3 activity and activated Drice were dramatically suppressed in *dark* homozygous mutant animals (Fig. 2I and L). Thus, Dark sits upstream of Drice, and mutation of *dark* prevents caspase-3 activation induced by polyglutamine. As mutants in Drice are not available, we were unable to determine whether caspase-3 activity is necessary for polyglutamine-induced cell death.

Given the dramatic effects of the *dark* mutation on cell death and caspase activation in the GMR-GAL4:UAS-Q108 eyes, we examined whether *dark* mutations might have similar effects in a more appropriate HD model that expresses polyglutamine within the context of human huntingtin. We examined TUNEL staining and activated Drice staining in adult retina expressing UAS-htt-exon1-Q93 under control of GMR-GAL4. In contrast to the dramatic rough eyes observed with UAS-Q108, the GMR-GAL4:UAS-htt-exon1-Q93 eyes were indistinguishable from GMR-GAL4 controls under the dissecting microscope (data not shown). Phalloidin staining of adult retina revealed that although remnants of ommatidial clusters were discernible, normal rhabdomere structures could not be identified in tangential optical sections (Fig. 2M). Longitudinal sections, however, revealed severe thinning of the retina, with extensive TUNEL staining evident in newly eclosed flies (Fig. 2O). In animals homozygous for mutant *dark* that expressed GMR-GAL4:UAS-httt-exon1-Q93, there was only mild rescue of the rhabdomere phenotype apparent in tangential sections (Fig. 2N), whereas more substantial rescue was apparent in longitudinal sections, with preservation of retinal thickness and complete suppression of TUNEL staining (Fig. 2P). We also examined activated Drice staining in tangential sections of whole mount retina. Extensive activated caspase staining was seen with GMR-GAL4:UAS-htt-exon1-Q93 (Fig. 2Q); this was completely suppressed in homozygous $dark^{CD4}$ mutant animals (Fig. 2R).

Dark inactivation suppresses formation and ubiquitination of polyglutamine aggregates

As aggregates of polyglutamine-containing proteins have been implicated in HD pathogenesis, we set out to assess the relationship between polyglutamine aggregates and Dark/Apaf-1. The localization of Q108 at different developmental stages was examined using an antibody (htt17) that detects the N-terminal of the Q108 construct. Punctate cytoplasmic aggregates were observed in photoreceptor clusters in both wild-type and homozygous $dark^{CD4}$ mutant eye discs isolated from developing third instar larvae expressing Q108 (Fig. 3B and C) but not in controls lacking Q108 (Fig. 3A). Shortly thereafter (at $\sim$10% pupal development), however, htt17 staining revealed numerous small cytoplasmic aggregates in all GMR-GAL4:UAS-Q108 photoreceptor neurons examined (arrowheads in Fig. 3E). Htt17 immunoreactivity often colocalized with anti-ubiquitin staining (arrowheads in Fig. 3H). Intranuclear ubiquitinated polyglutamine aggregates were identified in only a small number of photoreceptors ($<$5%), as evidenced by colocalization with the neuronal nuclear protein Elav (arrows in Fig. 3E, H, K and N). Condensed Elav staining was observed that likely represents pyknosis; in some instances this staining colocalized with nuclear Q108 (arrows in Fig. 3K and N). The control GMR-GAL4/+ eye did not show htt17 staining (Fig. 3D, G, J, M, and P).

The cellular localization of GMR-GAL4:UAS-Q108 was strikingly different in a homozygous $dark^{CD4}$ mutant background. Large cytoplasmic or nuclear aggregates were not observed. A uniform pattern of nuclear Elav staining was observed (Fig. 3L and O). More uniform cytoplasmic staining was seen using htt17, with negligible ubiquitin immunoreactivity (Fig. 3F, I, L and O). As GMR-GAL4:UAS-Q108 flies grew to a mid pupal stage, htt17 staining revealed the presence of accumulated cytoplasmic and perinuclear aggregates (arrowheads in Fig. 3Q). Lamellated oval structures containing actin filaments, Q108 and ubiquitin were observed (arrows in Fig. 3Q) (data not shown). These structures were not found in GMR-GAL4:UAS-Q108 eyes in a $dark^{CD4}$ homozygous mutant background, where htt17 staining remained more diffuse (Fig. 3R). These data suggest that Dark/Apaf-1 contributes, either directly or indirectly, to the growth of polyglutamine-containing aggregates.

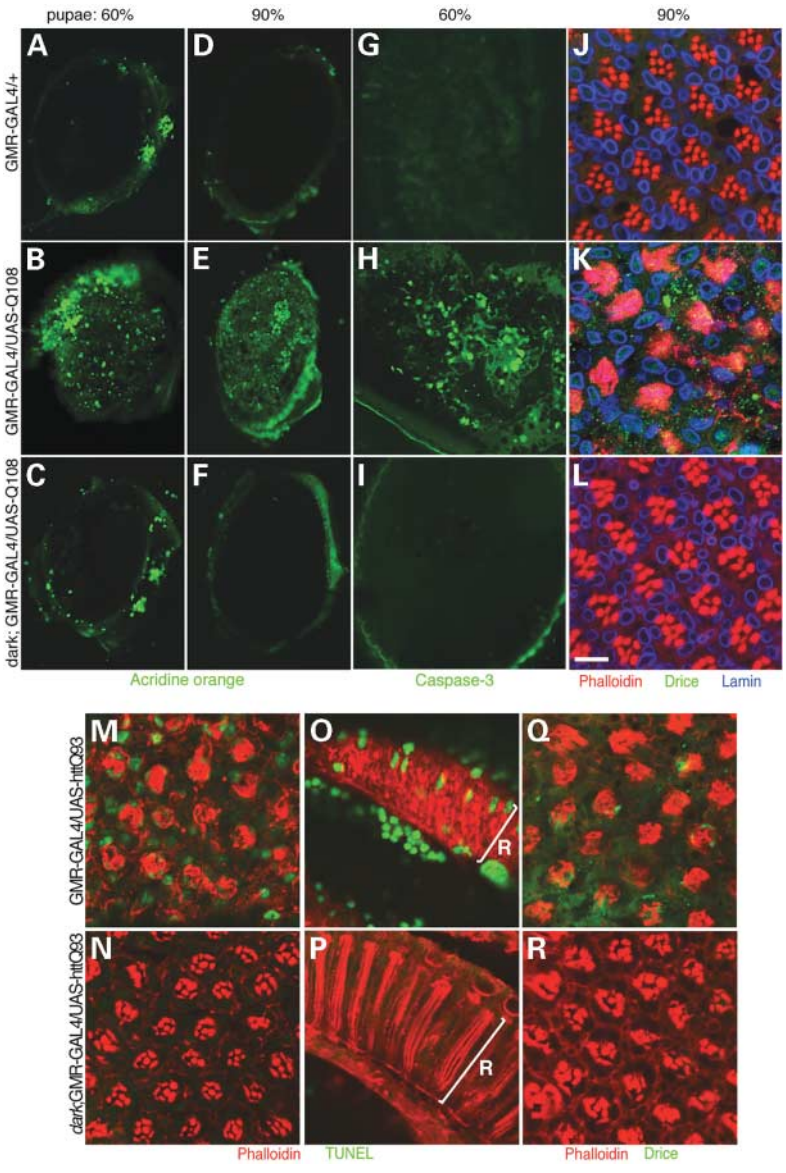

Figure 2. *dark* suppresses Q108 and mutant huntingtin exon1-induced cell death and caspase activation (**A**–**F**). Acridine orange staining of eyes at 60% (A–C) and 90% pupal development (D–F). (B and E) GMR-GAL4:UAS-Q108 eyes show widespread cell death during pupal development. Acridine orange staining of GMR-GAL4: UAS-Q108 in a homozygous mutant $dark^{CD4}$ background (C and F), is indistinguishable from the GMR-GAL4 control (A and D). Staining at the periphery of the eye results from damage incurred during dissection. (**G**–**I**) Caspase-3-like activity is detected *in situ* using a fluorigenic substrate in GMR-GAL4:UASQ108 eyes at 60% pupal development (H), but not in a homozygous $dark^{CD4}$ background (I) or in the GMR-GAL4 control (G). (**J**–**L**) Confocal images of 90% pupal eyes stained with phalloidin (red), anti-$Drice^{Active}$ (green) and anti-lamin Dm_0 (blue), which highlights the inner nuclear membrane. (K) Activated Drice is detected in degenerating GMR-GAL4:UAS-Q108 retina. (L) In a homozygous mutant $dark^{CD4}$ background, GMR-GAL4:UAS-Q108 shows normal retinal morphology with no detectable activated Drice, similar to the GMR-GAL4 control (J). (**M**–**P**) TUNEL labeling of newly eclosed adults shows extensive cell death in GMR-GAL4:UAS-httQ93 retina (M, tangential view; O, longitudinal view; green, TUNEL, red phalloidin). TUNEL staining was not observed in retina expressing GMR-GAL4/UAS-httQ93 in a homozygous $dark^{CD4}$ background, and longitudinal sections demonstrate dramatic rescue of retinal thickness (N, tangential view; P, longitudinal view). R indicates retinal layer in O, P. (**Q** and **R**) Activated Drice immunoreactivity is detected in GMR-GAL4:UAS-httQ93 eye (Q), but not in homozygous mutant $dark^{CD4}$ background (R). Scale bar: 10 μm (J–L). Genotypes: (A, D, G, and J), *w*; +; GMR-GAL4/+. (B, E, H, and K), *w*; +; GMR-GAL4/UAS-Q108-12. (C, F, I, and L), *w*; $dark^{CD4}$; GMR-GAL4/UAS-Q108-12.: (M, O, and Q), *w*; +; GMR-GAL4/UAS-htt-exon1-Q93. (N, P, and R), *w*; $dark^{CD4}$; GMR-GAL4/UAS-htt-exon1-Q93.

Mutation of *dark* suppresses adult onset polyglutamine-induced neurodegeneration

Neurodegeneration in HD occurs in the context of normally developed post-mitotic neurons. In the *Drosophila* retina, developmental aberrations can induce secondary neuronal cell death (55). Therefore, we set out to test whether Dark/Apaf-1 also exerts functions required for degeneration of adult neurons, perhaps more closely resembling that occurring in HD. We used a rhodopsin (Rh1)-GAL4 driver (56) to express

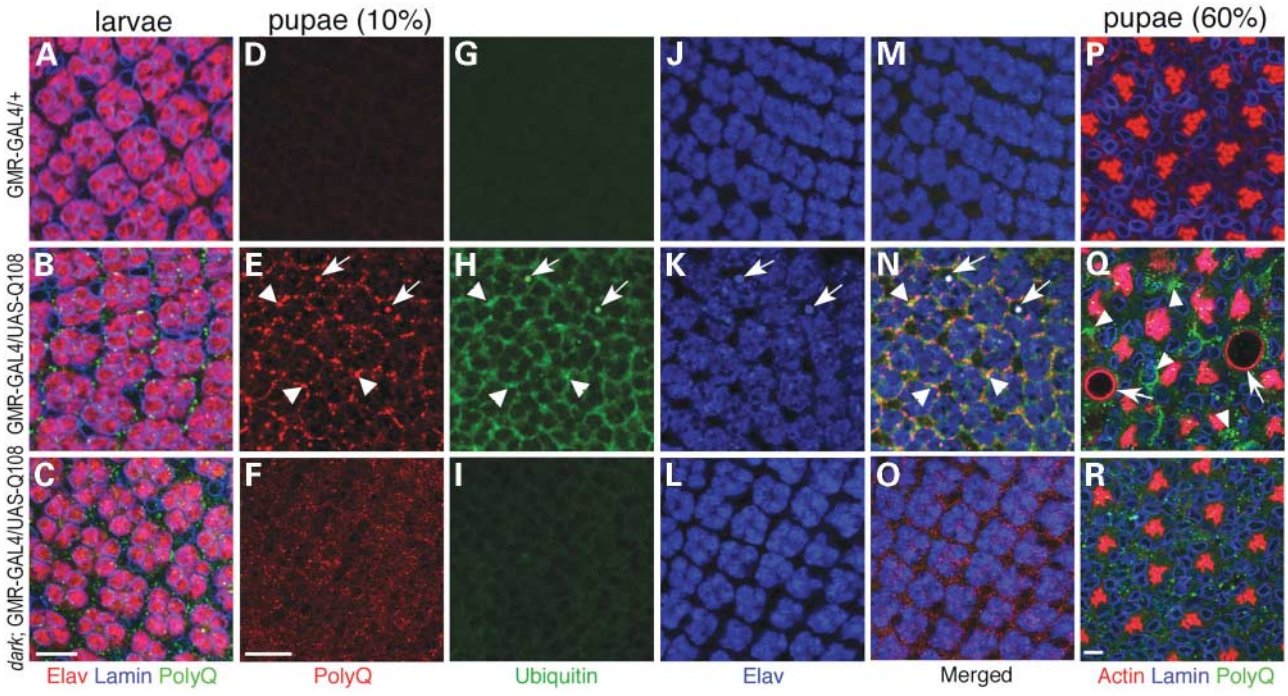

Figure 3. Accumulation of polyglutamine aggregates is suppressed by *dark* mutation. The upper panels (**A**, **D**, **G**, **J**, **M**, and **P**) show confocal images of GMR-GAL4/+ eyes, the middle panels (**B**, **E**, **H**, **K**, **N**, and **Q**) show images of GMR-GAL4:UAS-Q108 eyes and the lower panels show (**C**, **F**, **I**, **L**, **O**, and **R**) images of GMR-GAL4:UAS-Q108 in a $dark^{CD4}$ mutant background. (A–C) Confocal images of third instar larval eye discs stained with an antibody that recognizes the N-terminal of Q108 (green), anti-lamin Dm_0 (red) and anti-Elav (blue), a neuron-specific nuclear protein. Normal photoreceptor clusters with small cytoplasmic polyglutamine-containing aggregates are observed when GMR-GAL4:UAS-Q108 is expressed in wild-type (B) and homozygous $dark^{CD4}$ mutant backgrounds (C), whereas no polyglutamine signal is observed in the GMR-GAL4 control (A). (D–O) 10% pupal eye discs stained with anti-htt17 (red; D–F), anti-ubiquitin (green; G–I), anti-Elav (blue; **J**–**L**) and merged images of the three signals (M–O). In GMR-GAL4:UAS-Q108 eye (E, H, K, and N), polyglutamine aggregates frequently colocalized with ubiquitin (arrowheads), and some show unusually condensed Elav staining (arrows). In a homozygous $dark^{CD4}$ mutant background, the polyglutamine signal is more attenuated and dispersed (F), with barely detectable ubiquitin (I) and normal nuclear staining with anti-Elav (L). In the GMR-GAL4 control, normal Elav staining is observed with the absence of polyglutamine and ubiquitin signals (D, G, J, and M). (P–R) Late (60%) pupal eyes stained with phalloidin (red), anti-htt17 (green) and anti-lamin Dm_0 (blue). (Q) Disorganized ommatidial morphology with both cytoplasmic and perinuclear polyglutamine aggregates (arrowheads) and large actin-containing inclusions (arrows) are observed in eyes in which GMR-GAL4:UAS-Q108 is expressed. (R) A GMR-GAL4: UAS-Q108 eye in a mutant $dark^{CD4}$ background shows largely normal ommatidial morphology with punctate cytoplasmic polyglutamine aggregates. These small polyglutamine aggregates are similar to those seen earlier in development (C). Relatively normal ommatidial morphology other than mild abnormalities of polarity are observed for the GMR-GAL4 control (P). Scale bars: 10 μm (A–C), 15 μm (D–O), 5 μm (P–R). Genotypes: (A, D, G, J, M, and P), *w*; +; GMR-GAL4/+. (B, E, H, K, N, and Q), *w*; +; GMR-GAL4/UAS-Q108-12. (C, F, I, L, O, and R), *w*; $dark^{CD4}$; GMR-GAL4/UAS-Q108-12.

UAS-Q108 in R1–R6 photoreceptor neurons commencing late in pupal development. No abnormalities were observed in adult Rh1-GAL4:UAS-Q108 eyes at 1 week post-eclosion (data not shown). By 2 weeks, however, degeneration was apparent in some photoreceptors. R1–R6 photoreceptor degeneration was progressive, appearing more severe at 4 weeks, by which time phalloidin staining detected loss of rhabdomeres in Rh1-GAL4:UAS-Q108 eyes (Fig. 4B). Electron microscopy at this stage revealed collapsed rhabdomeres and extensive vacuolization in R1–R6 photoreceptor neurons. Many apoptotic features similar to those observed in GMR-GAL4:UAS-Q108 eyes, including condensed nuclei, electron dense cytoplasmic deposits and occasional 'dark' mitochondria and ER, were also detected (Fig. 4D). Ultrastructural features of central R7 photoreceptors, which do not express Rh1 or Q108, were normal (arrow in Fig. 4D). This observation argues for a cell autonomous mechanism of polyglutamine-induced cell death in this paradigm. By 8 weeks, massive R1–R6 photoreceptor degeneration was observed, whereas R7 cells remained intact (arrowheads in Fig. 4F). In contrast, in a mutant $dark^{CD4}$ background, the morphology of Rh1-GAL4:UAS-Q108 eyes at 4 weeks (Fig. 4C) was similar to wild-type (Fig. 4A). Ultrastructural analysis of Rh1-GAL4:UAS-Q108 eyes in a mutant $dark^{CD4}$ background at 4 weeks post-eclosion showed intact photoreceptor neurons without 'dark cell' features (Fig. 4E). Remarkably, even at 8 weeks, no significant abnormalities were observed in the phalloidin staining pattern of Rh1-GAL4:UAS-Q108 eyes in a homozygous $dark^{CD4}$ mutant background (Fig. 4G). We quantified the number of normal ommatidia in flies expressing Rh1-GAL4:UAS-Q108 in the presence and absence of *dark* at three different ages (Fig. 4H), demonstrating that adult onset, progressive neurodegeneration induced by Rh1-GAL4:UAS-Q108 was completely suppressed by a loss of function *dark* mutation. This profound suppressive effect of the *dark* mutation on Q108-induced cytotoxicity was not due to mutant *dark* induced changes in Rh1-dependent transcription (i.e. leading to a reduction in Q108 expression), as coexpression of an Rh1-GAL4-driven UAS-lacZ reporter was indistinguishable in wild-type and homozygous $dark^{CD4}$ mutant eyes (Supplementary Material, Fig. S3).

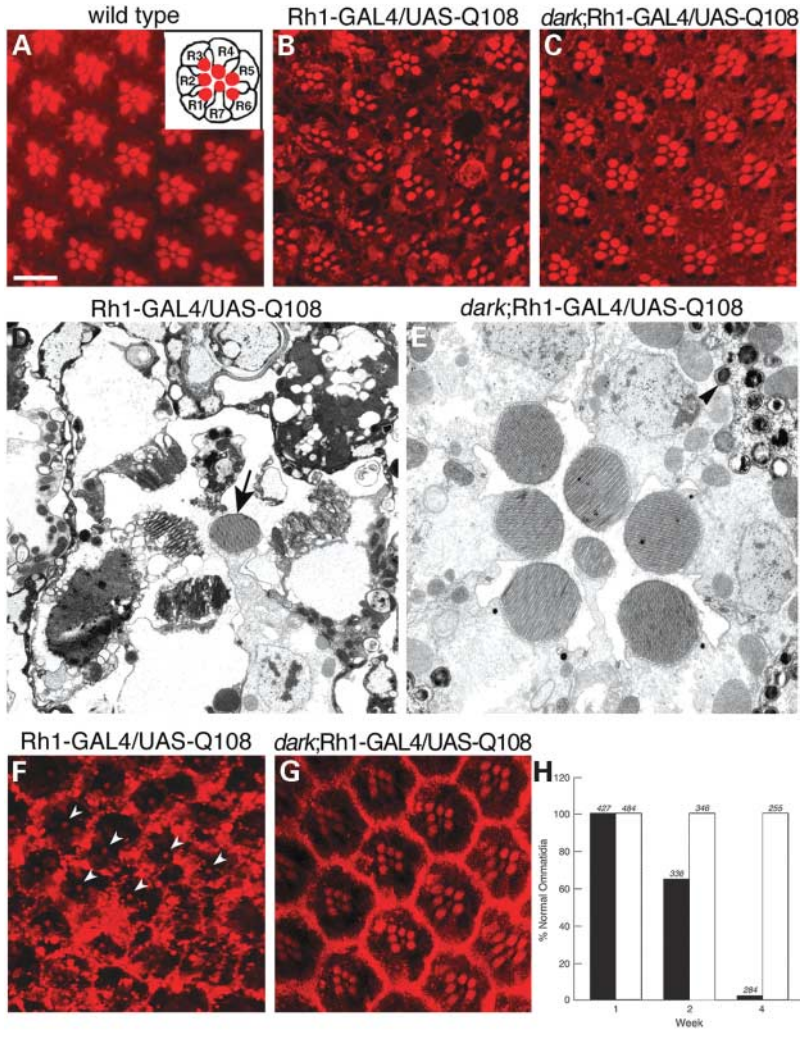

Figure 4. Late onset, progressive degeneration of outer photoreceptor neurons is suppressed by *dark*. UAS-Q108 was expressed under the control of a rhodopsin-GAL4 driver (Rh1-GAL4) expressed selectively in R1–R6 neurons commencing in late pupal development and persisting throughout adulthood. This provoked degeneration of R1–R6 neurons during adult life. (**A**–**C**) Confocal images of retina 4 weeks post-eclosion stained with phalloidin to highlight rhabdomeres. (A) In wild-type, rhabdomeres of each ommatidium are arranged in a trapezoidal pattern with six R1–R6 cells surrounding the central R7 cell (inset). (B) Rh1-GAL4:UAS-Q108 induces degeneration of R1–R6 cells (as assessed by the loss of rhabdomeres) in most ommatidia, whereas in R7 cells, which do not express Rh1, rhabdomeres remain intact (**D**). (C) Rh1-GAL4:UAS-Q108 in a mutant $dark^{CD4}$ background is largely wild-type. (D and **E**) Electron micrographs of retina at 4 weeks post-eclosion of Rh1-GAL4:UAS-Q108 in wild-type (D) and $dark^{CD4}$ backgrounds (E). (D) Tangential section of Rh1-GAL4:UAS-Q108 ommatidium shows electron dense, vacuolated R1–R6 photoreceptors with degenerated rhabdomere profiles, whereas R7 cells are normal (arrow). (E) In a $dark^{CD4}$ background, Rh1-GAL4:UAS-Q108 ommatidia show rhabdomeres arranged in a trapezoidal pattern with normal profiles. The electron dense bodies that contain pigment are normal structures (arrowhead). (**F** and **G**) Severe degeneration in animals aged 8 weeks post-eclosion is suppressed in a homozygous *dark* background. An 8 week-old eye stained with phalloidin (red). Rh1-GAL4:UAS-Q108 induces severe neurodegeneration in outer R cells, whereas R7 cells remain intact (F, arrowheads). In contrast, degeneration induced by Rh1-GAL4:UAS-Q108 is completely suppressed in homozygous $dark^{CD4}$ mutant animals (G). (H) Quantification of the number of normal ommatidia (i.e. those having the correct number and relative positions of R1–R7 cells) at weeks 1, 2 and 4 post-eclosion was carried out using phalloidin-stained preparations by confocal microscopy. For each genotype and time-point, at least 30 ommatidia were scored for each of 10–12 animals. Rh1-GAL4:UAS-Q108 (filled bar) induces progressive, age-dependent neurodegeneration, which is suppressed in a homozygous $dark^{CD4}$ background (open bar). Standard deviations were too small to appear on this graph. Scale bars: 10 μm (A, B, C, F and G). 2.5 μm (D and E). Genotypes: (A), Canton S. (B, D and F), *w*; +; Rh1-GAL4, UAS-lacZ/UAS-Q108-12. (C, E and G), *w*; $dark^{CD4}$; Rh1-GAL4, UAS-lacZ/UAS-Q108-12.

Mutation in *dark* suppresses neurodegeneration associated with polyglutamine expressed within a variety of protein contexts

Initially, we chose to assess effects of *dark* mutation on an extremely robust phenotype produced by expression of a polyglutamine peptide. In order to determine whether *dark* mutations also suppress neurodegeneration produced by polyglutamine within the context of disease-associated proteins, we set out to test *Drosophila* huntingtin exon 1 and full length ataxin-1 models. Similar to the approaches used to effect Q108 expression, UAS-huntingtin-exon1-Q93 (57) and UAS-ataxin-1-Q82 (58,59) transgenes were expressed using GMR- and Rh1-GAL4 drivers to generate early- and late-onset neurodegeneration, respectively. In the early-onset huntingtin model, expression of huntingtin-exon1-Q93 produced extensive

disruption of retinal morphology, as well as abnormal TUNEL and activated Drice staining (Fig. 2M, O and Q). When GMR-GAL4:UAS-htt-exon1-Q93 was expressed in a *dark* mutant background, TUNEL and Drice staining and the retinal degeneration phenotypes were improved (Fig. 2N, P and R).

In the late-onset huntingtin model, we observed numerous cytoplasmic and perinuclear aggregates stained with an anti-huntingtin antibody, EM48. This antibody preferentially recognizes mutant huntingtin-containing aggregates (60). The accumulation of these aggregates preceded any apparent degeneration (Fig. 5A and B). By 5 weeks post-eclosion, substantial retinal degeneration was observed; rhabdomeres were missing from the majority of ommatidia (Fig. 5C). Conversely, in a mutant $dark^{CD4}$ background, EM48 staining remained more diffuse, failing to produce large aggregates at the ages examined (Fig. 5D and E). Photoreceptor degeneration did not occur in the *dark* mutant background (Fig. 5F). Immunoblots using EM48 demonstrated that expression of mutant huntingtin was not suppressed in a $dark^{CD4}$ background (Supplementary Material, Fig. S4). UAS-ataxin-1-Q82 in *trans* to the strong GMR-GAL4 driver was semi-lethal at 23°C, however, at 18°C, a rough external phenotype was observed (Fig. 5G), which was largely suppressed in a $dark^{CD4}$ mutant background (Fig. 5H). When Rh1-GAL4 was used to drive UAS-ataxin-1-Q82, no photoreceptor loss was observed up to 6 weeks post-eclosion.

Dark accumulates in ubiquitinated protein aggregates

Our immunohistochemical studies demonstrated that *dark* mutation not only suppressed Q108-induced cell death but also blocked formation of large polyglutamine aggregates. These observations lead us to speculate that Dark might play a role in the development of pathogenic aggregates. Previous efforts have identified caspase-3 and possibly caspase-9, two components associated with the apoptosome (61), in intracellular aggregates in HEK293 cells expressing polyglutamine (62). We generated an antibody directed against Dark in order to study localization of the protein in the fly eye. Whole mount staining of GMR-GAL4:UAS-Q108 eyes showed that elevated levels of Dark protein colocalized with ubiquitinated aggregates (Fig. 6B), whereas this staining pattern was not observed in control eyes (Fig. 6C) or in GMR-GAL4:UAS-Q108 eyes stained with preimmune serum from animals prior to injection of the Dark peptide (Fig. 6A). Similar results were also obtained using mutant huntingtin exon1, where robust Dark aggregates were detected in GMR-GAL4:UAS-htt-exon1-Q93 retina (Fig. 6D), but not when this construct was expressed in a homozygous $dark^{CD4}$ mutant background (Fig. 6E).

Expanded polyglutamine enhances expression of Dark

Although Dark/Apaf-1 is required to activate the execution phase of certain caspase-dependent apoptotic pathways, its status under normal physiologic conditions has not been evaluated carefully. The observation that Dark immunoreactivity was increased in eyes expressing polyglutamine, but it was undetectable in wild-type controls, suggested that Dark may be induced or stabilized by polyglutamine expression. To test this hypothesis, we used immunoblotting to compare Dark levels in control and Q108-expressing eyes. Dark protein was abundant in GMR-GAL4:UAS-Q108 eyes but undetectable in normal eyes or in a $dark^{CD4}$ mutant background (compare lanes 1, 2, 3 in Fig. 7). In a $dark^{CD4}$ mutant background, the polyglutamine-induced increase in Dark protein was completely suppressed (lane 4 in Fig. 7).

Apaf-1 colocalizes with huntingtin aggregates in HD mice and patients

We next asked whether mammalian Apaf-1 also is associated with huntingtin aggregates. Caudate sections of R6/2 mice, which express a polyglutamine-expanded huntingtin exon 1 construct (63), from animals aged 3 months were stained with EM48 and Apaf-1 antibodies. Confocal microscopy demonstrated large nuclear EM48-immunoreactive aggregates, as well as punctate cytoplasmic aggregates (upper panels in Fig. 8A). Although Apaf-1 stained strongly in the cytoplasm, it also colocalized with nuclear EM48 signal in many cells (arrows in upper panels in Fig. 8A; and enlarged inset). A total of 72% (102/141) of EM48-positive nuclei also contained Apaf-1 signal. In age-matched control brain sections, there was a low level of Apaf-1 staining in scattered cells; EM48 staining was not observed (lower panels in Fig. 8A). We also observed Apaf-1 colocalized with aggregates as assessed using ubiquitin immunoreactivity in R6/2 brain sections (data not shown).

To investigate further the intriguing colocalization of Dark/Apaf-1 with polyglutamine aggregates in model systems, we tested whether Apaf-1 also is colocalized with huntingtin in HD patient brains. Caudate sections from three stage II HD brains (6) and three age-matched control brains were examined. EM48-immunoreactive huntingtin aggregates often colocalized with Apaf-1, as the merged image demonstrated (arrows in upper panels in Fig. 8B). There was also dispersed Apaf-1 immunoreactivity in HD brain that did not colocalize with huntingtin. Control samples showed occasional huntingtin immunoreactivity and less intense Apaf-1 signal (lower panel in Fig. 8B). The merged image did not show colocalization of huntingtin and Apaf-1. These convergent results from fly, mouse and man suggest that Dark/Apaf-1 may play a role in the formation of pathogenic polyglutamine-containing aggregates.

DISCUSSION

Proteins with abnormally expanded polyglutamine tracts have been linked to several neurodegenerative disorders, including HD. Here, we used a candidate-based genetic approach to evaluate potential modifiers and to define a role for Dark in polyglutamine-induced cell death. We demonstrated that a *dark* loss of function mutation strongly suppressed neurodegeneration, cell death and effector caspase activity in fly eyes expressing polyglutamine. In our experiments, we observed severe neurodegeneration with apoptotic and autophagic features, as well as the activation of caspase-3 and cell death in GMR-GAL4:UAS-Q108 eyes; these phenotypes were suppressed in a *dark* mutant background. We also used a late-onset model to demonstrate that mutation of *dark* can suppress progressive, age-dependent neurodegeneration. Moreover, the

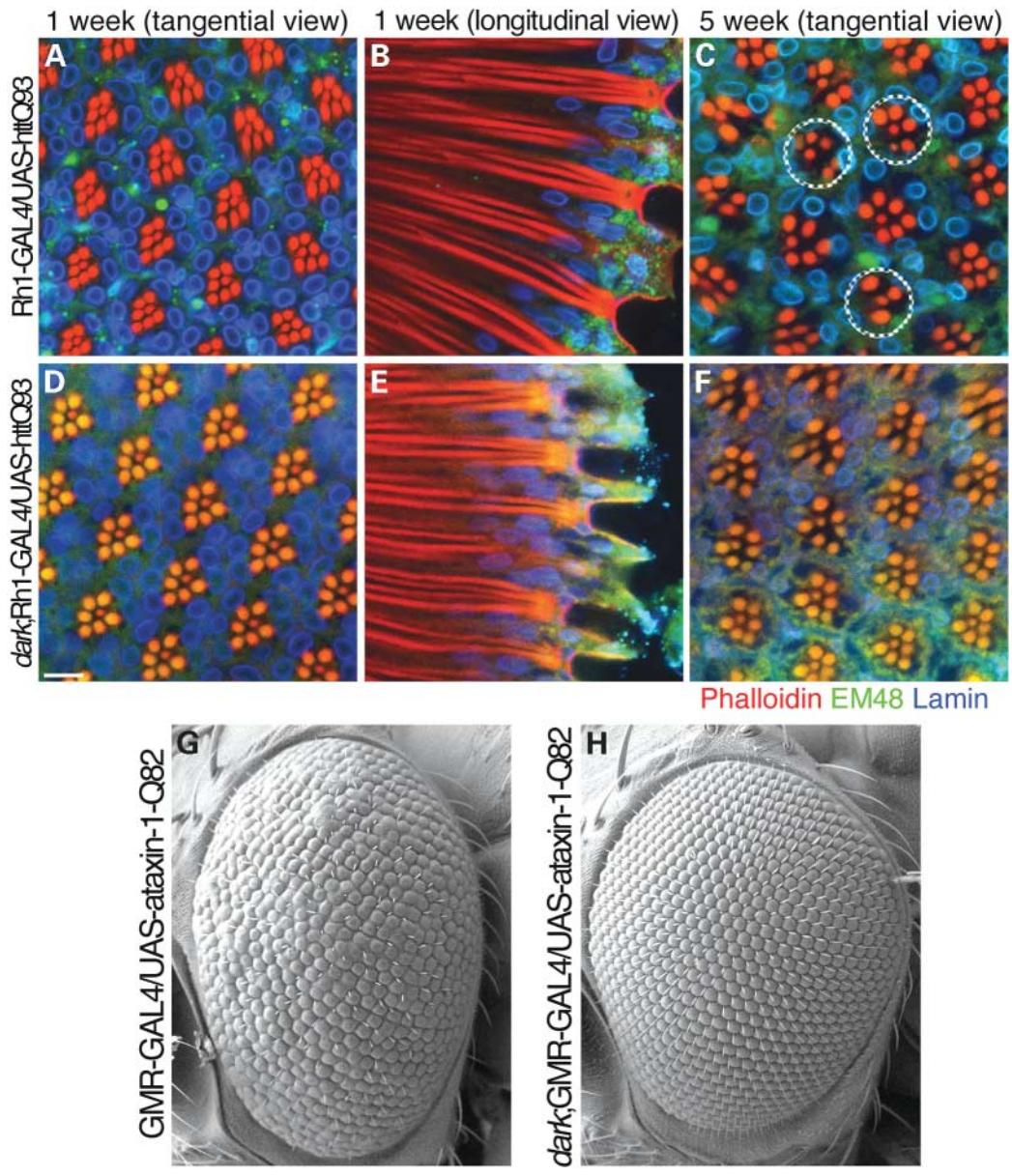

Figure 5. Mutation in *dark* suppresses mutant huntingtin exon1 and ataxin-1-induced neurodegeneration and aggregate formation. UAS-huntingtin-exon1-Q93 was expressed in R1–R6 photoreceptors under Rh1-GAL4 control (Rh1-GAL4:UAS-htt-Q93). Adult eyes were labeled with phalloidin (red), anti-huntingtin (EM48, green) and anti-Lamin Dm_0 (blue), and examined using confocal microscopy. (**A**–**C**) Rh1-GAL4:UAS-htt-Q93 eyes show normal rhabdomere organization in each ommatidium at 1 week. Nevertheless, many EM48-positive aggregates are detected (A, tangential view; B, longitudinal view). The degeneration of Rh1-GAL4:UAS-htt-Q93 eyes is progressive and can be detected at 3 week post-eclosion using phalloidin staining (data not shown). At 5 weeks, rhabdomere loss is apparent in most ommatidia, and the accumulation of EM48 immunoreactivity is evident (C; dashed circles show examples of ommatidia with degenerated rhabdomeres). Examination of Rh1-GAL4:UAS-htt-Q93 eyes at 1 week post-eclosion shows no obvious EM48-positive aggregates in a $dark^{CD4}$ mutant background (**D** and **E**), and age-dependent retinal degeneration is also suppressed. (**F**) A 5 week Rh1-GAL4: UAS-htt-Q93 eye in a $dark^{CD4}$ mutant background with normal morphology. (**G** and **H**) SEM images of GMR-GAL4:UAS-ataxin-1-Q82 eyes cultured at 18°C in the absence (G) or presence (H) of the $dark^{CD4}$ mutation show suppression of the rough eye phenotype by *dark* mutation. Scale bar: 100 μm. Genotypes: (A–C), *w*; +; Rh1-GAL4, UAS-lacZ/UAS-htt-exon1-Q93. (D–F), *w*; $dark^{CD4}$; Rh1-GAL4, UAS-lacZ/UAS-htt-exon1-Q93. (G), UAS-ataxin-1-Q82/+; +; GMR-GAL4/+. (H), UAS-ataxin-1-Q82; $dark^{CD4}$; GMR-GAL4/+.

suppressive effect of *dark* was also observed in *Drosophila* huntingtin exon 1 and full length ataxin-1 models. Both early- and adult-onset neurodegeneration induced by a mutant huntingtin fragment were suppressed by mutation of *dark.* A developmental rough eye phenotype caused by expression of mutant full length ataxin-1 was also suppressed when *dark* was inactivated.

We also found that mutation of *dark* suppressed polyglutamine aggregate accumulation, ubiquitination and nuclear localization. We demonstrated that Dark/Apaf-1 colocalized with disease protein in mouse and fly models, as well as patient brain, using immunohistochemical approaches. Dark protein appeared to be induced and/or stabilized by

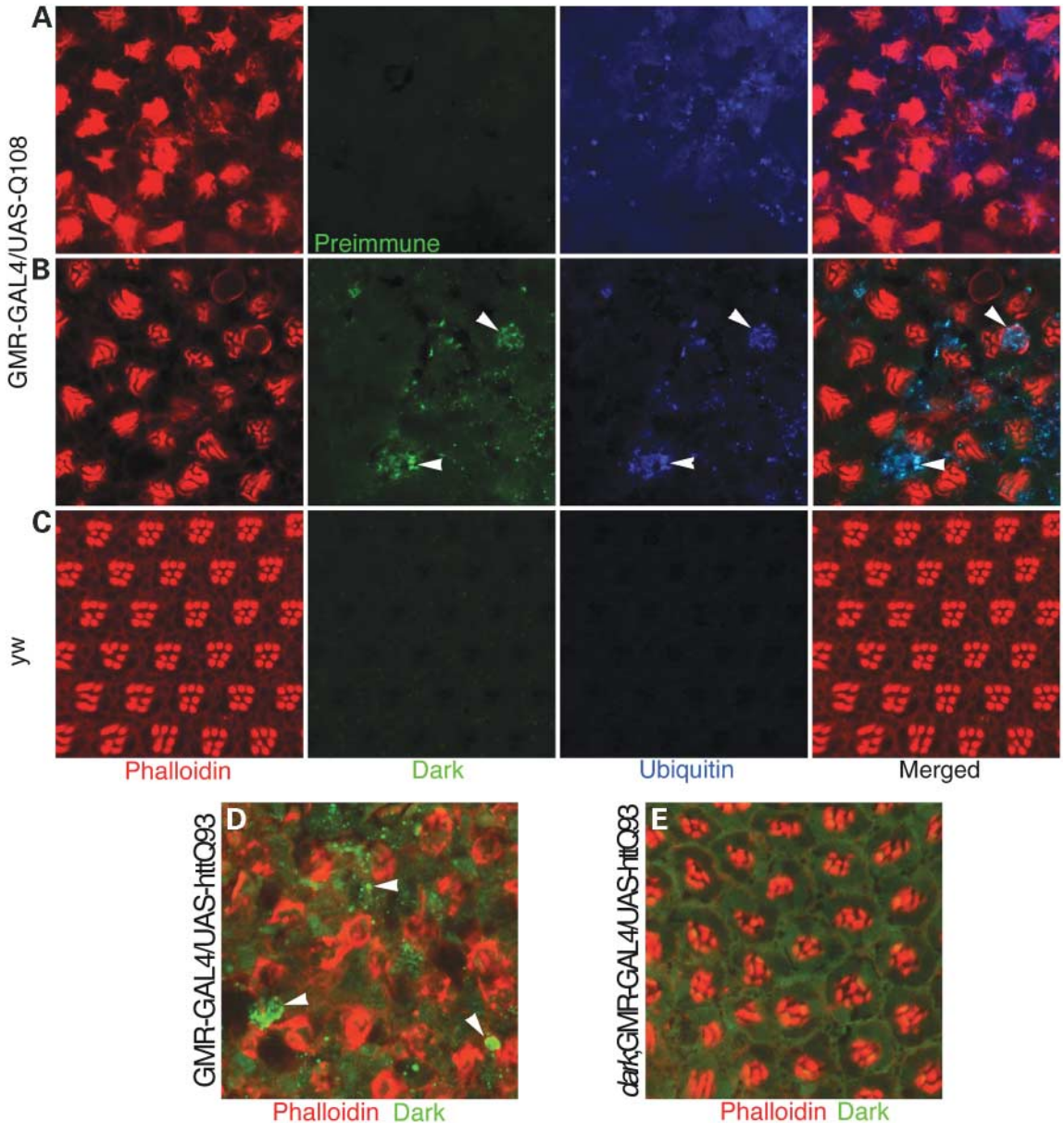

Figure 6. Localization of Dark in eyes expressing polyglutamine and mutant huntingtin. Late pupal eyes were triple labeled with phalloidin (red), preimmune serum (**A**) or anti-Dark (**B**, **C** and **D**; green) and anti-ubiquitin (blue) and examined using confocal microscopy. (A and B) GMR-GAL4:UAS-Q108 eyes show elevated anti-Dark immunoreactivity coinciding with ubiquitin (B, arrowheads). There is no detectable signal for preimmune serum (A). (C) *yw* (non-transgenic) control eyes show no immunoreactivity for either Dark or ubiquitin antibodies. (D and **E**) Confocal image shows a degenerated GMR-GAL4:UAS-httQ93 eye with elevated anti-Dark immunoreactivity including small aggregates (D, arrowheads), staining for UAS-Q93 in a $dark^{CD}$ mutant background remained diffuse (E). Red, phalloidin; green, anti-Dark.

polyglutamine expression *in vivo*. Together, these data demonstrate that Dark/Apaf-1 plays a key role in polyglutamine-induced neurodegeneration.

The question as to whether polyglutamine aggregates play a pivotal role in the pathogenesis of polyglutamine disorders is still unsettled, although a large body of evidence suggests that such aggregates are directly cytotoxic. However, considerable evidence also suggests that formation of polyglutamine-containing aggregates may be unrelated to cytoxicity or even protective. Ferrante *et al*. (64) have demonstrated a dissociation between the presence of huntingtin aggregates and the selective pattern of striatal neurodegeneration observed in HD brain. Zoghbi *et al.* (65) showed that transgenic mice expressing polyglutamine-expanded ataxin-1 with deletion of a self-association domain developed ataxia and Purkinje cell pathology in the absence of nuclear aggregates. Moreover, this same group examined the effects of polyglutamine-expanded ataxin-1 in mice deficient for the ubiquitin ligase E6-AP (66). Absence of the ubiquitin ligase delayed the appearance of nuclear aggregates but accelerated the development of ataxia and cerebellar neuropathology. Greenberg *et al.* (67) used a primary striatal culture model to show that

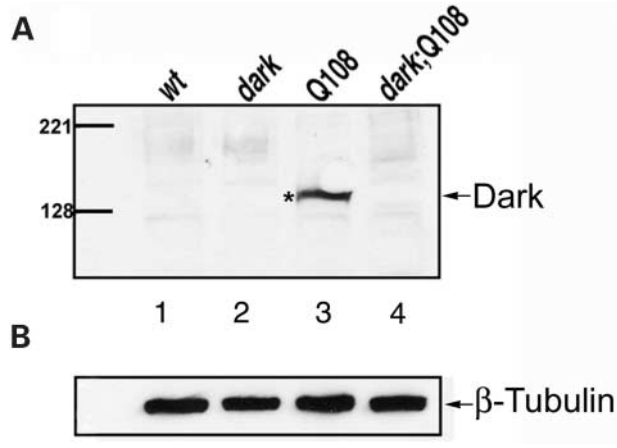

Figure 7. Induction of Dark protein by expanded polyglutamine. (**A**) Immunoblot analysis using a Dark antibody detects Dark expression in GMR-GAL4:UAS-Q108 (lane 3) but not in wild-type (lane 1), $dark^{CD4}$ (lane 2) or GMR-GAL4:UAS-Q108 extracts in a mutant $dark^{CD4}$ background (lane 4). Other experiments detected a faint band corresponding to Dark in extracts from aged wild-type heads (data not shown). (**B**) The same blot was stripped and then probed with anti-β-tubulin as a loading control.

interference with ubiquitin conjugation suppressed aggregation, but enhanced cytotoxicity of a mutant huntingtin fragment. More recently, Finkbeiner *et al.* (68) enlarged upon their earlier work by using real-time analysis of fluorescent aggregates in transfected striatal cultures to suggest that the presence of inclusion bodies correlated with improved survival. Although, none of these studies provide definitive resolution of the relationship between polyglutamine aggregation and toxicity, they do suggest a complex relationship between the two phenomena.

Here, we followed the development of polyglutamine aggregates in GMR-GAL4:UAS-Q108 eyes and evaluated aggregate formation in a *dark* mutant background. We observed, the evolution of polyglutamine staining from a punctate cytoplasmic pattern in young flies to large cytoplasmic and perinuclear aggregates in aged retina; some small fraction translocated into nuclei prior to the onset of degeneration and cell death. Conversely, Q108 expressed in a *dark* mutant background, in which polyglutamine staining remained cytoplasmic and more dispersed, never accumulated ubiquitin or gave rise to a neurodegenerative phenotype. Mutant huntingtin-containing aggregates also appeared prior to the onset of any detectable cell death in a late-onset paradigm, consistent with prior observations using a related late-onset fly model (26). These data support previous observations that the amelioration of mutant huntingtin phenotypes by various inhibitors is accompanied by decreased aggregate formation (32–35). Recently, Wetzel and coworkers (69) used synthetic polyglutamine aggregates directly applied to PC12 cells to demonstrate that polyglutamine aggregates are cytotoxic. These authors also showed that peptides that inhibit polyglutamine fibril elongation could successfully suppress cytotoxicity. The data presented here support this conclusion and further suggest that Dark/Apaf-1 activity is a determinant of polyglutamine aggregate development and toxicity.

A simple means of evaluating a role of apoptotic pathways in *Drosophila* degenerative phenotypes is to express the broad spectrum caspase inhibitor p35 (49). Early studies of polyglutamine-associated neurodegeneration in *Drosophila* found either no effect (26) or poor suppression (70) with p35. We found no effect of p35 coexpression on GMR-GAL4:UAS-Q108 (data not shown). Despite lack of efficacy of p35 for polyglutamine and huntingtin exon1 phenotypes in retina, mutation of *dark* reversed cell death and Drice activation in response to these constructs. How can these observations be reconciled? p35-insensitive caspases are thought to initiate cell death in insect Sf9 cells (71). The initiator caspase Dronc, which shows some similarity to caspase-9 and might be expected to complex with Dark in a fly apoptosome, is insensitive to p35 (50,72), although conflicting results have been reported (48). That dominant negative Dronc transgenes do not suppress the GMR-GAL4:UAS-Q108 phenotype may reflect a need for more pronounced inhibition than that achieved using a dominant negative transgene. Finally, it is not clear that Drice is p35-sensitive; indeed, there are indications that Drice may cleave and thus inactivate p35 (73,74). Faber *et al.* (75) have reported that mutant huntingtin-induced cell death and abnormal morphology are partially suppressed by mutations of CED-3, the worm caspase homolog. Moreover, CED-3 appears to play an important but non-essential role in the formation of polyglutamine aggregates. These results using a *C. elegans* model are similar to those reported here, although the suppression observed in the worm was less dramatic than that observed in the fly. The lack of caspase redundancy in *C. elegans* as opposed to *Drosophila melanogaster* may account for the suppression observed by CED-3 mutation as opposed to the negative results obtained here using p35 overexpression and manipulation of Dronc and Dredd. However, caspase-independent roles of CED-4/Dark have been described recently in both worm and fly (76,77). The data presented here provide a platform for further evaluation of the relationships between polyglutamine toxicity, Dark/Apaf-1 and caspases.

Dark/Apaf-1 colocalized with polyglutamine aggregates, raising the intriguing possibility that Apaf-1 plays a role in aggregate accumulation in HD brains. What is the connection between polyglutamine and Dark/Apaf1? A schematic depicting a proposed role of Dark/Apaf-1 in polyglutamine pathogenesis in the fly retina is shown in Figure 8C. According to this model, as a consequence of mutant huntingtin-induced transcriptional dysregulation, p53 is induced (78). This in turn results in induction of Dark; Apaf-1 is a well-known transcriptional target of p53 (79). Recent work has revealed a set of molecular interactions that may further link polyglutamine and Dark/Apaf-1. CED-4, the worm homolog of Dark, associates with *C. elegans* MAC-1 (80), an AAA ATPase that is homologous to mammalian VCP. VCP binds to polyglutamine *in vitro* (81), and loss of function of *TER94*, the fly homolog of VCP, suppresses polyglutamine-induced neurodegeneration *in vivo* (82). It is intriguing to note that missense mutations in VCP have been associated recently with another dominant degenerative disease, inclusion body myopathy with Paget's disease of bone and frontotemporal dementia (83). The molecular chaperone hsp70, which suppresses polyglutamine-induced cell death in flies (84), may exert its effect by direct

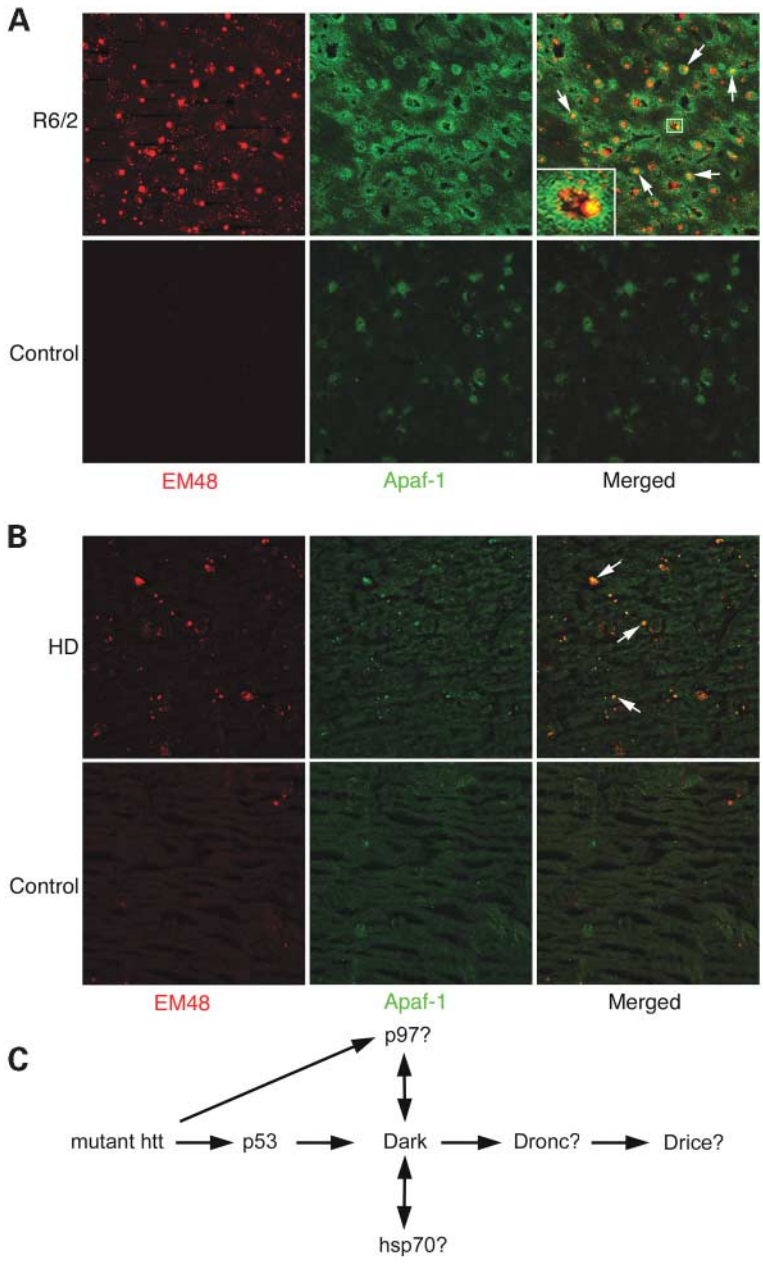

Figure 8. Apaf-1 immunoreactivity in huntingtin aggregates of HD transgenic mice and human HD brain. (**A**) Cryostat sections of 3 month-old R6/2 mouse striatum (upper panels) and non-transgenic age-matched controls (lower panels) were immunolabeled with EM48 (red) and Apaf-1 antibodies (green). Upper panels show that EM48-positive nuclear aggregates in R6/2 brain often colocalize with elevated Apaf-1 immunoreactivity, as evidenced by the merged image (arrows and enlarged inset). Lower panel shows that no EM48 signal is observed in control striatum, and Apaf-1 staining is less intensed and more dispersed (compare green signal of upper panel with lower panel). (**B**) Paraffin sections of stage II HD striatum (upper panels) and age-matched controls (lower panels) were immunolabeled with EM48 (red) and Apaf-1 antibodies (green). Upper panels shows that huntingtin aggregates often colocalize with Apaf-1, as demonstrated in the merged image (arrows). There is also dispersed Apaf-1 immunoreactivity in HD brain that does not colocalize with huntingtin. Control striatum in lower panels shows occasional huntingtin staining and negligible Apaf-1 signal. The merged image does not show colocalization of huntingtin and Apaf-1. (**C**) A schematic depicting a proposed role of Dark/Apaf-1 in polyglutamine pathogenesis.

association with Apaf-1 to block apoptosis (85,86), or to block aggregate accumulation and thus suppress toxicity. These studies suggest that Dark/Apaf-1 occupies a crucial position in pathways leading to aggregation and toxicity associated with polyglutamine disease. Other identified modifiers, including VCP and chaperonins, may function by regulating the activity of Apaf-1 and formation of the apoptosome complex. Reducing *dark* activity effectively reverses polyglutamine pathogenesis *in vivo* from an early stage; polyglutamine expression continues, but cells are able to effectively cope with mutant protein without undergoing cell death. Our data cannot distinguish whether the observed suppression of aggregate formation observed with *dark* inactivation indicates a direct relationship between Dark and aggregation or whether

inhibition of aggregation with *dark* inactivation occurs owing to a profound, but nonetheless unrelated, early suppression of cell death. Genetic epistasis experiments to address this question are underway. Nonetheless, our findings suggest Apaf-1 might effectively be targeted as an early preventive or disease-modifying therapy for HD, and such efforts may be expected to have effects on both pathologic protein aggregation and cell death, two crucial aspects of neurodegenerative disease that are reiterated in *Drosophila* retinal models.

MATERIALS AND METHODS

Drosophila genetics

Standard genetic markers and chromosomes were used as described (87). All experiments were carried out at room temperature unless otherwise noted. For analysis of *dark* and *dredd* loss of function mutations, a strong third chromosome UAS-Q108 transgenic line was placed in *trans* to GMR-GAL4 (88). Although many GMR-GAL4 inserts have markedly abnormal rough eye phenotypes (89) in the absence of a UAS target gene, the phenotypes associated with the GMR-GAL4 used in these studies were weak. p35 and dominant negative Dronc constructs were tested for their ability to rescue a phenotype induced by a Q108 insertion in the second chromosome. Transgene expression in the presence of *dark* mutations was performed by crossing stocks maintained over the attached double balancer T (2;3) SM6, TM6B. Use of the joined double balancer permitted unequivocal identification of genotypes in larvae and pupae. The *null* dark alleles were obtained by imprecise excision of the $dark^{CD4}$ line (47). A similar scheme was used for adult-onset expression, except that Rh1-GAL4, UAS-lacZ chromosome was used rather than GMR-GAL4.

Electron microscopy

Analysis of adult eye phenotypes by scanning electron microscopy was carried out as described previously (90), except that (with the exception of experiments using ataxin-1) fresh anesthetized rather than dehydrated specimens were used. Flies were prepared for transmission electron microscopy as described previously (91). Samples were observed using a JEOL JEM-100 CX II electron microscope.

Immunohistochemistry

The affinity-purified rabbit polyclonal antibody directed against a peptide corresponding to the N-terminal 17 amino acids of human huntingtin was generated commercially (Bethyl Laboratories) and used at 1:100 for immunohistochemistry. This antibody was found to react with the Q108 peptide in immunohistochemistry. The rabbit Dark antiserum, raised against a peptide (QLEREQKRRRSRRH) corresponding to Dark residues 1267–1280, was generated by Alpha Diagnostics. Whole mount staining of larval and pupal eye discs and adult retinas was carried out as described previously (26,90,91). Samples were analyzed on a Bio-Rad confocal microscope. For acridine orange and caspase-3 activity assays, larval and pupal eye discs were dissected without fixation. *In situ* caspase-3 activity was determined using Phi-PhiLux reagent (Oncoimmunin), according to a modification of a previous application to the eye disc (92). Acridine orange and phalloidin-TRITC were obtained from Sigma. Alexifluor 647-conjugated phalloidin was from Molecular Probes. Primary antibodies were anti-ubiquitin (1:100, Zymed), mouse EM48 (1:50, Chemicon), rat anti-Elav (1:100), rabbit polyclonal or mouse anti-lamin Dm_0 (1:200), rabbit anti-activated Drice (1:50) and anti-Apaf-1 (Stressgen; 1:100). Secondary fluorochrome-conjugated antibodies included FITC, TRITC and Cy3 (1:100, Jackson Immunoresearch). TUNEL staining was carried out using the *In Situ* Cell Death Detection Kit (fluorescein) according to the manufacturer's instructions (Roche).

R6/2 mice that express exon 1 of human huntingtin-containing 115–150 CAG repeats (64) were obtained from Jackson Laboratories. Immunohistochemical evaluation was carried out on cryostat sections of R6/2 and control striatum aged 3 months.

Human brain samples from three neuropathological grade II (6) HD patients and three age-matched controls were obtained from the Harvard Brain Tissue Resource Center. Two grade III brain samples were also used. Caudate/putamen and cortical regions were examined. Brains were collected by the brain bank 9–16 h post-mortem from neurologically characterized cases and embedded in paraffin.

Quantitation of cell death in adult retina

Photoreceptor loss in adults expressing Rh1-GAL4:UAS-Q108 was quantified by loss of rhabdomeres staining with phalloidin-Alexifluor 647 in whole mount retinas. For each genotype and time-point, at least 30 ommatidia were scored for each of 10–12 animals.

Immunoblotting

For immunoblot analysis of Dark protein, extracts from heads of the following genotypes: (1) Canton S (wild-type), (2) *yw*; $dark^{CD4}$, (3) *w*; +; GMR-GAL4/UAS-Q108 and (4) *w*; $dark^{CD4}$; GMR-GAL4/UAS-Q108 were obtained and resolved by 7.5% SDS–PAGE. For lacZ immunoblotting, protein extraction was performed from *Drosophila* retinas of the following genotypes: (1) *w*; +; Rh1-GAL4, UAS-lacZ/UAS-Q108 and (2) *w*; *dark*; Rh1-GAL4, UAS-lacZ/UAS-Q108. Retinas were dissected out and resolved by 12% SDS–PAGE. For EM48 immunoblotting, extracts from heads of the following genotypes were analyzed using a 5–20% gradient gel: (1) Canton S, (2) *w*; +; Rh1-GAL4, UAS-lacZ/UAS-huntingtin-Q93 and (3) *w*; $dark^{CD4}$; Rh1-GAL4, UAS-lacZ/UAS-huntingtin-Q93. Immunoblots were developed with peroxidase-conjugated secondary antibody and enhanced chemiluminescence. Antibody dilutions were as follows: mouse anti-β-galactosidase (Roche; 1:1000), rabbit anti-Dark (1:3000), mouse anti-EM48 (Chemicon; 1:2000) and mouse anti-β-tubulin (Accurate Science; 1:1000).

SUPPLEMENTARY MATERIAL

Supplementary Material is available at HMG Online.

ACKNOWLEDGEMENTS

The authors would like to thank Birgitta Sjöstrand for assistance with TEM, Leslie Thompson and Larry Marsh for the UAS-Q108 and UAS-huntingtin-Q93 fly stocks, Mel Feany for the UAS-ataxin-1-Q82 stock, Pascal Meier for the UAS-Dronc^{C318A} and UAS-Dronc^{CARD} stocks, the Bloomington Stock Center for miscellaneous fly stocks, the Developmental Hybridoma Studies Bank maintained by the University of Iowa for the Elav antibody, Bruce Hay for the activated Drice antibody and Paul Fisher for the anti-lamin Dm_0 antibodies. Thanks also to Carl Johnson and Iris Salecker for critical comments on the manuscript, and to George Lawless for excellent technical assistance. S.L.Z. is an investigator of the Howard Hughes Medical Institute. The authors also would like to express their gratitude to John Mazziotta and Peter Whybrow for their generous support of the UCLA Neurogenetics Program and the Center for Neurobehavioral Genetics. This work was supported by NS002116 and V54 ES012078 (G.R.J.), AG012466 (J.M.A.) and the Cure HD Initiative (G.R.J. and C.L.) and a John J. Wasmuth Postdoctoral Fellowship (T.-K.S.) of the Hereditary Disease Foundation.

REFERENCES

1. Folstein, S.E. (1989) *Huntington's Disease: A Disorders of Families*. Johns Hopkins University Press, Baltimore.
2. Bates, G. (2003) Huntingtin aggregation and toxicity in Huntington's disease. *Lancet*, **361**, 1642–1644.
3. Young, A.B. (2003) Huntingtin in health and disease. *J. Clin. Invest*, **111**, 299–302.
4. Albin, R.L. (2003) Dominant ataxias and Friedreich ataxia: an update. *Curr. Opin. Neurol.*, **16**, 507–514.
5. Zoghbi, H.Y. and Orr, H.T. (2000) Glutamine repeats and neurodegeneration. *Annu. Rev. Neurosci.*, **23**, 217–247.
6. Vonsattel, J.P., Myers, R.H., Stevens, T.J., Ferrante, R.J., Bird, E.D. and Richardson, E.P., Jr (1985) Neuropathological classification of Huntington's disease. *J. Neuropathol. Exp. Neurol.*, **44**, 559–577.
7. DiFiglia, M., Sapp, E., Chase, K.O., Davies, S.W., Bates, G.P., Vonsattel, J.P. and Aronin, N. (1997) Aggregation of huntingtin in neuronal intranuclear inclusions and dystrophic neurites in brain. *Science*, **277**, 1990–1993.
8. Sapp, E., Schwarz, C., Chase, K., Bhide, P.G., Young, A.B., Penney, J., Vonsattel, J.P., Aronin, N. and DiFiglia, M. (1997) Huntingtin localization in brains of normal and Huntington's disease patients. *Ann. Neurol.*, **42**, 604–612.
9. Hermel, E., Gafni, J., Propp, S.S., Leavitt, B.R., Wellington, C.L., Young, J.E., Hackam, A.S., Logvinova, A.V., Peel, A.L., Chen, S.F. *et al.* (2004) Specific caspase interactions and amplification are involved in selective neuronal vulnerability in Huntington's disease. *Cell Death Differ.*, **11**, 424–438.
10. Kim, Y.J., Yi, Y., Sapp, E., Wang, Y., Cuiffo, B., Kegel, K.B., Qin, Z.-H., Aronin, N. and DiFiglia, M. (2001) Caspase 3-cleaved N-terminal fragments of wild-type and mutant huntingtin are present in normal and Huntington's disease brains, associate with membranes, and undergo calpain-dependent proteolysis. *Proc. Natl Acad. Sci. USA*, **98**, 12784–12789.
11. Sanchez, I., Xu, C.J., Juo, P., Kakizaka, A., Blenis, J. and Yuan, J. (1999) Caspase-8 is required for cell death induced by expanded polyglutamine repeats. *Neuron*, **22**, 623–633.
12. Wellington, C.L., Ellerby, L.M., Hackam, A.S., Margolis, R.L., Trifiro, M.A., Singaraja, R., McCutcheon, K., Salvesen, G.S., Propp, S.S., Bromm, M. *et al.* (1998) Caspase cleavage of gene products associated with triplet expansion disorders generates truncated fragments containing the polyglutamine tract. *J. Biol. Chem.*, **273**, 9158–9167.
13. Ellerby, L.M., Andrusiak, R.L., Wellington, C.L., Hackam, A.S., Propp, S.S., Wood, J.D., Sharp, A.H., Margolis, R.L., Ross, C.A., Salvesen, G.S. *et al.* (1999) Cleavage of atrophin-1 at caspase site aspartic acid 109 modulates cytotoxicity. *J. Biol. Chem.*, **274**, 8730–8736.
14. Kim, M., Lee, H.S., LaForet, G., McIntyre, C., Martin, E.J., Chang, P., Kim, T.W., Williams, M., Reddy, P.H., Tagle, D. *et al.* (1999) Mutant huntingtin expression in clonal striatal cells: dissociation of inclusion formation and neuronal survival by caspase inhibition. *J. Neurosci.*, **19**, 964–973.
15. Moulder, K.L., Onodera, O., Burke, J.R., Strittmatter, W.J. and Johnson, E.M., Jr (1999) Generation of neuronal intranuclear inclusions by polyglutamine-GFP: analysis of inclusion clearance and toxicity as a function of polyglutamine length. *J. Neurosci.*, **19**, 705–715.
16. Miyashita, T., Matsui, J., Ohtsuka, Y., Mami, U., Fujishima, S., Okamura-Oho, Y., Inoue, T. and Yamada, M. (1999) Expression of extended polyglutamine sequentially activates initiator and effector caspases. *Biochem. Biophys. Res. Commun.*, **257**, 724–730.
17. Wang, G.H., Mitsui, K., Kotliarova, S., Yamashita, A., Nagao, Y., Tokuhiro, S., Iwatsubo, T., Kanazawa, I. and Nukina, N. (1999) Caspase activation during apoptotic cell death induced by expanded polyglutamine in N2a cells. *Neuroreport*, **10**, 2435–2438.
18. Li, S.H., Lam, S., Cheng, A.L. and Li, X.J. (2000) Intranuclear huntingtin increases the expression of caspase-1 and induces apoptosis. *Hum. Mol. Genet.*, **9**, 2859–2867.
19. Jana, N.R., Zemskov, E.A., Wang, G. and Nukina, N. (2001) Altered proteasomal function due to the expression of polyglutamine-expanded truncated N-terminal huntingtin induces apoptosis by caspase activation through mitochondrial cytochrome *c* release. *Hum. Mol. Genet.*, **10**, 1049–1059.
20. U, M., Miyashita, T., Ohtsuka, Y., Okamura-Oho, Y., Shikama, Y. and Yamada, M. (2001) Extended polyglutamine selectively interacts with caspase-8 and -10 in nuclear aggregates. *Cell Death Differ.*, **8**, 377–386.
21. LaFevre-Bernt, M.A. and Ellerby, L.M. (2003) Kennedy's disease. Phosphorylation of the polyglutamine-expanded form of androgen receptor regulates its cleavage by caspase-3 and enhances cell death. *J. Biol. Chem.*, **278**, 34918–34924.
22. Huynh, D.P., Yang, H.T., Vakharia, H., Nguyen, D. and Pulst, S.M. (2003) Expansion of the polyQ repeat in ataxin-2 alters its Golgi localization, disrupts the Golgi complex and causes cell death. *Hum. Mol. Genet.*, **12**, 1485–1496.
23. Sanchez, I., Mahlke, C. and Yuan, J. (2003) Pivotal role of oligomerization in expanded polyglutamine neurodegenerative disorders. *Nature*, **421**, 373–379.
24. Chen, M., Ona, V.O., Li, M., Ferrante, R.J., Fink, K.B., Zhu, S., Bian, J., Guo, L., Farrell, L.A., Hersch, S.M. *et al.* (2000) Minocycline inhibits caspase-1 and caspase-3 expression and delays mortality in a transgenic mouse model of Huntington disease. *Nat. Med.*, **6**, 797–801.
25. Ona, V.O., Li, M., Vonsattel, J.P., Andrews, L.J., Khan, S.Q., Chung, W.M., Frey, A.S., Menon, A.S., Li, X.J., Stieg, P.E. *et al.* (1999) Inhibition of caspase-1 slows disease progression in a mouse model of Huntington's disease. *Nature*, **399**, 263–267.
26. Jackson, G.R., Salecker, I., Dong, X., Yao, X., Arnheim, N., Faber, P.W., MacDonald, M.E. and Zipursky, S.L. (1998) Polyglutamine-expanded human huntingtin transgenes induce degeneration of *Drosophila* photoreceptor neurons. *Neuron*, **21**, 633–642.
27. Bonini, N.M. and Fortini, M.E. (2003) Human neurodegenerative disease modeling using *Drosophila*. *Annu. Rev. Neurosci.*, **26**, 627–656.
28. Yamamoto, A., Lucas, J.J. and Hen, R. (2000) Reversal of neuropathology and motor dysfunction in a conditional model of Huntington's disease. *Cell*, **101**, 57–66.
29. Carmichael, J., Chatellier, J., Woolfson, A., Milstein, C., Fersht, A.R. and Rubinsztein, D.C. (2000) Bacterial and yeast chaperones reduce both aggregate formation and cell death in mammalian cell models of Huntington's disease. *Proc. Natl Acad. Sci. USA*, **97**, 9701–9705.
30. Jana, N.R., Tanaka, M., Wang, G. and Nukina, N. (2000) Polyglutamine length-dependent interaction of Hsp40 and Hsp70 family chaperones with truncated N-terminal huntingtin: their role in suppression of aggregation and cellular toxicity. *Hum. Mol. Genet.*, **9**, 2009–2018.
31. Wyttenbach, A., Carmichael, J., Swartz, J., Furlong, R.A., Narain, Y., Rankin, J. and Rubinsztein, D.C. (2000) Effects of heat shock, heat shock protein 40 (HDJ-2), and proteasome inhibition on protein aggregation in cellular models of Huntington's disease. *Proc. Natl Acad. Sci. USA*, **97**, 2898–2903.
32. Kazantsev, A., Walker, H.A., Slepko, N., Bear, J.E., Preisinger, E., Steffan, J.S., Zhu, Y.Z., Gertler, F.B., Housman, D.E., Marsh, J.L. *et al.* (2002) A bivalent Huntingtin binding peptide suppresses polyglutamine aggregation and pathogenesis in *Drosophila*. *Nat. Genet.*, **30**, 367–376.

33. Murphy, R.C. and Messer, A. (2004) A single-chain Fv intrabody provides functional protection against the effects of mutant protein in an organotypic slice culture model of Huntington's disease. *Brain Res. Mol. Brain Res.*, **121**, 141–145.
34. Pollitt, S.K., Pallos, J., Shao, J., Desai, U.A., Ma, A.A., Thompson, L.M., Marsh, J.L. and Diamond, M.I. (2003) A rapid cellular FRET assay of polyglutamine aggregation identifies a novel inhibitor. *Neuron*, **40**, 685–694.
35. Tanaka, M., Machida, Y., Niu, S., Ikeda, T., Jana, N.R., Doi, H., Kurosawa, M., Nekooki, M. and Nukina, N. (2004) Trehalose alleviates polyglutamine-mediated pathology in a mouse model of Huntington disease. *Nat. Med.*, **10**, 148–154.
36. Marsh, J.L., Walker, H., Theisen, H., Zhu, Y.Z., Fielder, T., Purcell, J. and Thompson, L.M. (2000) Expanded polyglutamine peptides alone are intrinsically cytotoxic and cause neurodegeneration in *Drosophila*. *Hum. Mol. Genet.*, **9**, 13–25.
37. Rodriguez, A., Oliver, H., Zou, H., Chen, P., Wang, X. and Abrams, J.M. (1999) Dark is a *Drosophila* homologue of Apaf-1/CED-4 and functions in an evolutionarily conserved death pathway. *Nat. Cell Biol.*, **1**, 272–279.
38. Adams, J.M. and Cory, S. (2002) Apoptosomes: engines for caspase activation. *Curr. Opin. Cell Biol.*, **14**, 715–720.
39. Kanuka, H., Sawamoto, K., Inohara, N., Matsuno, K., Okano, H. and Miura, M. (1999) Control of the cell death pathway by Dapaf-1, a *Drosophila* Apaf-1/CED-4-related caspase activator. *Mol. Cell*, **4**, 757–769.
40. Zhou, L., Song, Z., Tittel, J. and Steller, H. (1999) HAC-1, a *Drosophila* homolog of APAF-1 and CED-4 functions in developmental and radiation-induced apoptosis. *Mol. Cell*, **4**, 745–755.
41. Brand, A.H. and Perrimon, N. (1993) Targeted gene expression as a means of altering cell fates and generating dominant phenotypes. *Development*, **118**, 401–415.
42. Turmaine, M., Raza, A., Mahal, A., Mangiarini, L., Bates, G.P. and Davies, S.W. (2000) Nonapoptotic neurodegeneration in a transgenic mouse model of Huntington's disease. *Proc. Natl Acad. Sci. USA*, **97**, 8093–8097.
43. Yu, Z.-X., Li, S.-H., Evans, J., Pillarisetti, A., Li, H. and Li, X.-J. (2003) Mutant huntingtin causes context-dependent neurodegeneration in mice with Huntington's disease. *J. Neurosci.*, **23**, 2193–2202.
44. Kerr, J.F., Wyllie, A.H. and Currie, A.R. (1972) Apoptosis: a basic biological phenomenon with wide-ranging implications in tissue kinetics. *Br. J. Cancer*, **26**, 239–257.
45. Kegel, K.B., Kim, M., Sapp, E., McIntyre, C., Castano, J.G., Aronin, N. and DiFiglia, M. (2000) Huntingtin expression stimulates endosomal–lysosomal activity, endosome tubulation, and autophagy. *J. Neurosci.*, **20**, 7268–7278.
46. Qin, Z.-H., Wang, Y., Kegel, K.B., Kazantsev, A., Apostol, B.L., Thompson, L.M., Yoder, J., Aronin, N. and DiFiglia, M. (2003) Autophagy regulates the processing of amino terminal huntingtin fragments. *Hum. Mol. Genet.*, **12**, 3231–3244.
47. Rodriguez, A. (2002) Genetic and molecular analysis of programmed cell death in *Drosophila*. UT Southwestern Medical Center, thesis.
48. Quinn, L.M., Dorstyn, L., Mills, K., Colussi, P.A., Chen, P., Coombe, M., Abrams, J., Kumar, S. and Richardson, H. (2000) An essential role for the caspase dronc in developmentally programmed cell death in *Drosophila*. *J. Biol. Chem.*, **275**, 40416–40424.
49. Hay, B.A., Wolff, T. and Rubin, G.M. (1994) Expression of baculovirus P35 prevents cell death in *Drosophila*. *Development*, **120**, 2121–2129.
50. Meier, P., Silke, J., Leevers, S.J. and Evan, G.I. (2000) The *Drosophila* caspase DRONC is regulated by DIAP1. *EMBO J.*, **19**, 598–611.
51. Chen, P., Rodriguez, A., Erskine, R., Thach, T. and Abrams, J.M. (1998) Dredd, a novel effector of the apoptosis activators reaper, grim, and hid in *Drosophila*. *Dev. Biol.*, **201**, 202–216.
52. Leulier, F., Rodriguez, A., Khush, R.S., Abrams, J.M. and Lemaitre, B. (2000) The *Drosophila* caspase Dredd is required to resist gram-negative bacterial infection. *EMBO Rep.*, **1**, 353–358.
53. Abrams, J.M., White, K., Fessler, L.I. and Steller, H. (1993) Programmed cell death during *Drosophila* embryogenesis. *Development*, **117**, 29–43.
54. Dorstyn, L., Read, S., Cakouros, D., Huh, J.R., Hay, B.A. and Kumar, S. (2002) The role of cytochrome *c* in caspase activation in *Drosophila* melanogaster cells. *J. Cell Biol.*, **156**, 1089–1098.
55. Bonini, N.M. and Fortini, M.E. (1999) Surviving *Drosophila* eye development: integrating cell death with differentiation during formation of a neural structure. *Bioessays*, **21**, 991–1003.
56. Chyb, S., Hevers, W., Forte, M., Wolfgang, W.J., Selinger, Z. and Hardie, R.C. (1999) Modulation of the light response by cAMP in *Drosophila* photoreceptors. *J. Neurosci.*, **19**, 8799–8807.
57. Steffan, J.S., Bodai, L., Pallos, J., Poelman, M., McCampbell, A., Apostol, B.L., Kazantsev, A., Schmidt, E., Zhu, Y.Z., Greenwald, M. *et al.* (2001) Histone deacetylase inhibitors arrest polyglutamine-dependent neurodegeneration in *Drosophila*. *Nature*, **413**, 739–743.
58. Feany, M.B. and Bender, W.W. (2000) A *Drosophila* model of Parkinson's disease. *Nature*, **404**, 394–398.
59. Fernandez-Funez, P., Nino-Rosales, M.L., de Gouyon, B., She, W.C., Luchak, J.M., Martinez, P., Turiegano, E., Benito, J., Capovilla, M., Skinner, P.J. *et al.* (2000) Identification of genes that modify ataxin-1-induced neurodegeneration. *Nature*, **408**, 101–106.
60. Gutekunst, C.A., Li, S.H., Yi, H., Mulroy, J.S., Kuemmerle, S., Jones, R., Rye, D., Ferrante, R.J., Hersch, S.M. and Li, X.J. (1999) Nuclear and neuropil aggregates in Huntington's disease: relationship to neuropathology. *J. Neurosci.*, **19**, 2522–2534.
61. Bratton, S.B., Walker, G., Roberts, D.L., Cain, K. and Cohen, G.M. (2001) Caspase-3 cleaves Apaf-1 into an ~30 kDa fragment that associates with an inappropriately oligomerized and biologically inactive ~1.4 MDa apoptosome complex. *Cell Death Differ.*, **8**, 425–433.
62. Suhr, S.T., Senut, M.C., Whitelegge, J.P., Faull, K.F., Cuizon, D.B. and Gage, F.H. (2001) Identities of sequestered proteins in aggregates from cells with induced polyglutamine expression. *J. Cell Biol.*, **153**, 283–294.
63. Mangiarini, L., Sathasivam, K., Seller, M., Cozens, B., Harper, A., Hetherington, C., Lawton, M., Trottier, Y., Lehrach, H., Davies, S.W. *et al.* (1996) Exon 1 of the HD gene with an expanded CAG repeat is sufficient to cause a progressive neurological phenotype in transgenic mice. *Cell*, **87**, 493–506.
64. Kuemmerle, S., Gutekunst, C.A., Klein, A.M., Li, X.J., Li, S.H., Beal, M.F., Hersch, S.M. and Ferrante, R.J. (1999) Huntingtin aggregates may not predict neuronal death in Huntington's disease. *Ann. Neurol.*, **46**, 842–849.
65. Klement, I.A., Skinner, P.J., Kaytor, M.D., Yi, H., Hersch, S.M., Clark, H.B., Zoghbi, H.Y. and Orr, H.T. (1998) Ataxin-1 nuclear localization and aggregation: role in polyglutamine-induced disease in SCA1 transgenic mice. *Cell*, **95**, 41–53.
66. Cummings, C.J., Reinstein, E., Sun, Y., Antalffy, B., Jiang, Y., Ciechanover, A., Orr, H.T., Beaudet, A.L. and Zoghbi, H.Y. (1999) Mutation of the E6-AP ubiquitin ligase reduces nuclear inclusion frequency while accelerating polyglutamine-induced pathology in SCA1 mice. *Neuron*, **24**, 879–892.
67. Saudou, F., Finkbeiner, S., Devys, D. and Greenberg, M.E. (1998) Huntingtin acts in the nucleus to induce apoptosis but death does not correlate with the formation of intranuclear inclusions. *Cell*, **95**, 55–66.
68. Arrasate, M., Mitra, S., Schweitzer, E.S., Segal, M.R. and Finkbeiner, S. (2004) Inclusion body formation reduces levels of mutant huntingtin and the risk of neuronal death. *Nature*, **431**, 805–810.
69. Thakur, A.K., Yang, W. and Wetzel, R. (2004) Inhibition of polyglutamine aggregate cytotoxicity by a structure-based elongation inhibitor. *FASEB J.* **18**, 923–925.
70. Warrick, J.M., Paulson, H.L., Gray-Board, G.L., Bui, Q.T., Fischbeck, K.H., Pittman, R.N. and Bonini, N.M. (1998) Expanded polyglutamine protein forms nuclear inclusions and causes neural degeneration in *Drosophila*. *Cell*, **93**, 939–949.
71. Manji, G.A. and Friesen, P.D. (2001) Apoptosis in motion. An apical, P35-insensitive caspase mediates programmed cell death in insect cells. *J. Biol. Chem.*, **276**, 16704–16710.
72. Hawkins, C.J., Yoo, S.J., Peterson, E.P., Wang, S.L., Vernooy, S.Y. and Hay, B.A. (2000) The *Drosophila* caspase DRONC cleaves following glutamate or aspartate and is regulated by DIAP1, HID, and GRIM. *J. Biol. Chem.*, **275**, 27084–27093.
73. Fraser, A.G. and Evan, G.I. (1997) Identification of a *Drosophila* melanogaster ICE/CED-3-related protease, drICE. *EMBO J.*, **16**, 2805–2813.

74. Fraser, A.G., McCarthy, N.J. and Evan, G.I. (1997) drICE is an essential caspase required for apoptotic activity in *Drosophila* cells. *EMBO J.*, **16**, 6192–6199.
75. Faber, P.W., Alter, J.R., MacDonald, M.E. and Hart, A.C. (1999) Polyglutamine-mediated dysfunction and apoptotic death of a *Caenorhabditis elegans* sensory neuron. *Proc. Natl Acad. Sci. USA*, **96**, 179–184.
76. Bloss, T.A., Witze, E.S. and Rothman, J.H. (2003) Suppression of CED-3-independent apoptosis by mitochondrial betaNAC in *Caenorhabditis elegans*. *Nature*, **424**, 1066–1071.
77. Huh, J.R., Vernooy, S.Y., Yu, H., Yan, N., Shi, Y., Guo, M. and Hay, B.A. (2004) Multiple apoptotic caspase cascades are required in nonapoptotic roles for *Drosophila* spermatid individualization. *PLoS Biol.*, **2**, E15.
78. Steffan, J.S., Kazantsev, A., Spasic-Boskovic, O., Greenwald, M., Zhu, Y.Z., Gohler, H., Wanker, E.E., Bates, G.P., Housman, D.E. and Thompson, L.M. (2000) The Huntington's disease protein interacts with p53 and CREB-binding protein and represses transcription. *Proc. Natl Acad. Sci. USA*, **97**, 6763–6768.
79. Fortin, A., Cregan, S.P., MacLaurin, J.G., Kushwaha, N., Hickman, E.S., Thompson, C.S., Hakim, A., Albert, P.R., Cecconi, F., Helin, K. *et al.* (2001) APAF1 is a key transcriptional target for p53 in the regulation of neuronal cell death. *J. Cell Biol.*, **155**, 207–216.
80. Wu, D., Chen, P.J., Chen, S., Hu, Y., Nuñez, G. and Ellis, R.E. (1999) C. elegans MAC-1, an essential member of the AAA family of ATPases, can bind CED-4 and prevent cell death. *Development*, **126**, 2021–2031.
81. Hirabayashi, M., Inoue, K., Tanaka, K., Nakadate, K., Ohsawa, Y., Kamei, Y., Popiel, A.H., Sinohara, A., Iwamatsu, A., Kimura, Y. *et al.* (2001) VCP/p97 in abnormal protein aggregates, cytoplasmic vacuoles, and cell death, phenotypes relevant to neurodegeneration. *Cell Death Differ.*, **8**, 977–984.
82. Higashiyama, H., Hirose, F., Yamaguchi, M., Inoue, Y.H., Fujikake, N., Matsukage, A. and Kakizuka, A. (2002) Identification of ter94, *Drosophila* VCP, as a modulator of polyglutamine-induced neurodegeneration. *Cell Death Differ.*, **9**, 264–273.
83. Watts, G.D., Wymer, J., Kovach, M.J., Mehta, S.G., Mumm, S., Darvish, D., Pestronk, A., Whyte, M.P. and Kimonis, V.E. (2004) Inclusion body myopathy associated with Paget disease of bone and frontotemporal dementia is caused by mutant valosin-containing protein. *Nat. Genet.*, **36**, 377–381.
84. Warrick, J.M., Chan, H.Y., Gray-Board, G.L., Chai, Y., Paulson, H.L. and Bonini, N.M. (1999) Suppression of polyglutamine-mediated neurodegeneration in *Drosophila* by the molecular chaperone HSP70. *Nat. Genet.*, **23**, 425–428.
85. Saleh, A., Srinivasula, S.M., Balkir, L., Robbins, P.D. and Alnemri, E.S. (2000) Negative regulation of the Apaf-1 apoptosome by Hsp70. *Nat. Cell Biol.*, **2**, 476–483.
86. Beere, H.M., Wolf, B.B., Cain, K., Mosser, D.D., Mahboubi, A., Kuwana, T., Tailor, P., Morimoto, R.I., Cohen, G.M. and Green, D.R. (2000) Heat-shock protein 70 inhibits apoptosis by preventing recruitment of procaspase-9 to the Apaf-1 apoptosome. *Nat. Cell Biol.*, **2**, 469–475.
87. Lindsley, D. and Zimm, G.G. (1992) *The Genome of Drosophila melanogaster.* Academic Press, San Diego.
88. Patel, P.H., Thapar, N., Guo, L., Martinez, M., Maris, J., Gau, C.L., Lengyel, J.A. and Tamanoi, F. (2003) *Drosophila* Rheb GTPase is required for cell cycle progression and cell growth. *J. Cell Sci.*, **116**, 3601–3610.
89. Freeman, M. (1996) Reiterative use of the EGF receptor triggers differentiation of all cell types in the *Drosophila* eye. *Cell*, **87**, 651–660.
90. Jackson, G.R., Wiedau-Pazos, M., Sang, T.K., Wagle, N., Brown, C.A., Massachi, S. and Geschwind, D.H. (2002) Human wild-type tau interacts with wingless pathway components and produces neurofibrillary pathology in *Drosophila*. *Neuron*, **34**, 509–519.
91. Sang, T.K. and Ready, D.F. (2002) Eyes closed, a *Drosophila* p47 homolog, is essential for photoreceptor morphogenesis. *Development*, **129**, 143–154.
92. Kanuka, H., Hisahara, S., Sawamoto, K., Shoji, S., Okano, H. and Miura, M. (1999) Proapoptotic activity of *Caenorhabditis elegans* CED-4 protein in *Drosophila*: implicated mechanisms for caspase activation. *Proc. Natl Acad. Sci. USA*, **96**, 145–150.